The Effects of Multiple Companions on the Efficiency of the SIM Planet Searches

Eric B. Ford[1]

Astronomy Department, 601 Campbell Hall, University of California at Berkeley, Berkeley, CA 94720-3411, USA

Department of Astrophysical Sciences, Princeton University, Peyton Hall, Princeton, NJ 08544-1001, USA

`eford@astron.berkeley.edu`

ABSTRACT

The Space Interferometry Mission (SIM) is expected to make precise astrometric measurements that can be used to detect low mass planets around nearby stars. Since most nearby stars are members of multiple star systems, many stars will have a measurable acceleration due to their companion, which must be included when solving for astrometric parameters and searching for planetary perturbations. Additionally, many of the stars with one radial velocity planet show indications of additional planets. Therefore, astrometric surveys like SIM must be capable of detecting planets and measuring orbital parameters in systems with multiple stellar and/or planetary companions. We have conducted Monte Carlo simulations to investigate how the presence of multiple companions affects the sensitivity of an astrometric survey such as SIM. We find that the detection efficiency for planets in wide binary systems is relatively unaffected by the presence of a binary companion, if the planetary orbital period is less than half the duration of the astrometric survey. For longer orbital periods, there are significant reductions in the sensitivity of an astrometric survey. Additionally, we find that the signal required to detect a planet can be increased significantly due to the presence of an additional planet orbiting the same star. Fortunately, adding a modest number of precision radial velocity observations significantly improves the sensitivity for many multiple planet systems. Thus, the combination of radial velocity observations and astrometric observations by SIM will be a particularly valuable for studying multiple planet systems.

Subject headings: planetary systems – techniques: interferometric

---

[1]Miller Research Fellow

1.   Introduction

During the last decade, high precision radial velocity surveys have discovered $\sim$170 planets orbiting nearby stars (Butler *et al.* 2002 and references therein; http://exoplanets.org; http://www.obspm.fr/planets). Many of the planets orbit stars believed to be members of wide binary systems ($\sim$ 1000 AU; Eggenberger, Udry, & Mayor 2004), and nearly $\sim$ 20 of the stars with one radial velocity planet have at least one additional companion. Additionally, there are indications that many more stars with planets show residuals suggestive of additional planets (Fischer *et al.* 2001).

Astrometric planet searches could provide valuable information about nearby planetary systems and planets in multiple star systems. While radial velocity measurements are only capable of measuring $m \sin i$, the mass of a planet times the inclination of its orbital plane to the plane of the sky, astrometric observations measure both the mass and inclination separately. Accurate masses and inclinations are important for dynamical analyses of multiple planet systems. (e.g., Ford, Lystad, & Rasio 2005; Lee & Peale 2002). For example, classical planet formation theory predicts that planets form on nearly coplanar orbits. Astrometric measurements of multiple planet systems could test this prediction.

Similarly, astrometric planet searches could yield insight into possible differences in the planets around single and binary stars. For example, Zucker & Mazeh (2002) claim to detect a mass-period correlation and that it is different for planets around single stars and planets around one star in a binary system. There are also theoretical reasons to believe that planetary systems may be affected in binary systems. For example, it is now believed that dynamical interactions between a planet and a wide binary companion can result in significant evolution of a planet's orbit. In systems such as 16 Cygni, the distant stellar companion (16 Cyg A) may be responsible for large oscillations in the orbital eccentricity of a planet around 16 Cyg B (Holman, Touma, & Tremaine 1997). More speculatively, some have proposed that distant binary companions might even produce giant planets with orbital periods of $\sim 1 - 4$ d, that are difficult to produce in conventional theories of planet formation. If the orbital plane of the stellar binary and the orbital plane of the planet are nearly perpendicular, then secular interactions can result in very large eccentricity oscillations and a planet reaching a periastron of only a few stellar radii. In such a case, tidal dissipation might result in a planet's orbit becoming circularized with a semi-major axis of several stellar radii (Ford, Rasio, & Sills 1998; Faber, Rasio, & Willems 2004; Takeda & Rasio 2005).

The Space Interferometry Mission (SIM) will make precision astrometric measurements suitable for detecting planets around nearby stars (Marcy *et al.* 2005; Sozzetti 2005). Two of the key projects are surveys to search for low-mass planets (Marcy *et al.* 2002; Shao *et al.* 2002), many of which are likely to be in multiple planet systems or wide stellar binary systems. Therefore, it is important to understand how the sensitivity of an astrometric planet search is impacted by the presence of multiple planets and wide binary systems. Additionally, SIM is expected to conduct follow up observations of some planetary systems discovered by radial velocity surveys. If giant planets serve as tracers of planetary systems containing low-mass planets, then these follow up observations

could also yield new detections of low-mass planets in planetary systems also containing one or more giant planets. Given that such solar-system analogues would be very exciting, it is important to understand the sensitivity of SIM to multiple planet systems.

Similarly, since we know that most nearby stars are members of binary star systems, it is important to understand how a wide binary companion would affect the sensitivity of SIM to planetary companions. If the acceleration due to a distant companion were to interfere with SIM's ability to detect low mass planets, then it might be prudent to remove stars with binary companions from the SIM target list in favor of more distant single stars. Alternatively, if SIM is able to detect low mass planets equally well around single stars and stars in wide binary systems, then it would be desirable to target the closest stars whether or not they are in binaries. Targeting both single and binary stars could provide information about how the formation of planetary systems differs between these two types of stars. Previously, Sozzetti *et al.* (2002) and Ford & Tremaine (2003) have investigated the sensitivity of SIM for detecting a single planet around a star and measuring its mass and orbital parameters. Additionally, Sozetti *et al.* (2003) have begun to investigate the potential of SIM for detecting and characterizing multiple planet systems. They concentrate on giant planets and use the known radial velocity systems as a guide. This study considers SIM planet searches for two-planet systems more generally. In particular, we focus on how the sensitivity of SIM to lower mass planets is affected by the presence of an addition planet.

In this paper, we explore the sensitivity of astrometric surveys for detecting and characterizing the orbits of planets in multiple planet systems or in wide binaries. While we have chosen simulation parameters to approximate the planned SIM narrow-angle planet searches, many of our simulation results can be rescaled for various measurement precisions, planet masses, and stellar distances which can be of use for other astrometric planet searches, such as those being planned for PRIMA and GAIA. Further, our conclusions should be qualitatively applicable to most astrometric planet searches. We summarize our assumptions and methods in §2. In §3 we present the results of our simulations for planets in binaries systems. In §4 we describe the particular model for planets in multiple planet systems and address several specific questions regarding the discovery potential of SIM for two-planet systems. In §5, we show how the addition of radial velocity measurements can increase the sensitivity of SIM to certain types of multiple planet systems. Finally, we summarize our main findings and conclusions in §6.

2. Methods

We simulate astrometric observations following the method of Ford (2004). For each star we simulate $2N_{obs} = 48$ (for $P_{SD} = 5$ years) or $2N_{obs} = 96$ (for $P_{SD} = 10$ years) one dimensional astrometric observations grouped in pairs. The N_{obs} observation times (t_i) are distributed over the survey duration P_{SD}. Each pair of observations occurs nearly simultaneously and is made with perpendicular baselines. A Gaussian noise source with standard deviation σ_{SIM} is added to each one dimensional observation. We used the "periodic with perturbations" observing schedule

(with $\epsilon = 0.2$) discussed in Ford (2004). In this schedule the observation times are periodic, except that Gaussian perturbations with standard deviation $\epsilon P_{SD}/N_{obs} \simeq 15$ d have been applied to the time of each observation, to reduce the effects of aliasing near the orbital period $P_{SD}/N_{obs} = 76$ d. While the simulations of Ford (2004) demonstrated the merits of this observing schedule, that study was restricted to observing schedules that were not able to use information obtained from early observations for the scheduling of future observations.

One way in which SIM's eventual sensitivity might be improved is by the application of adaptive scheduling algorithms that use of early observations to improve the scheduling of later observations, such as proposed by Loredo (2004). Ford (2005b) developed computationally feasible algorithms for radial velocity surveys and demonstrated that adaptive scheduling algorithms could significantly improve the efficiency of radial velocity planet searches. It would be straightforward (but computationally demanding) to implement similar adaptive scheduling algorithms for astrometric surveys, potentially increasing the efficiency of SIM planet searches. Due to the larger number of parameters required to describe the astrometric motion of an isolated star (position, parallax, and proper motion as compared to only the line-of-sight radial velocity), we expect that a somewhat larger number of early observations will be necessary before the benefits of adaptive scheduling become significant. We expect that future studies will implement adaptive scheduling algorithms for astrometric searches and evaluate their performance characteristics. In this study, we restrict our attention to fixed observing schedules, primarily due to the demanding computational requirements of such adaptive scheduling algorithms, especially given that we must simulate millions of planetary systems to explore the very large parameter space necessary to describe multiple planet systems.

For SIM's narrow angle planet surveys, each "single measurement" of a target star will consist of multiple measurements of the optical path length delay for the target star and multiple nearby reference stars while maintaining the spacecraft orientation. Each pair of optical path length delay measurements for two different stars results in a relative delay measurements between the target star and a reference stars. This one dimensional relative delay measurement is proportional to the the angular distance between the two stars projected onto the interferometer baseline (Marcy *et al.* 2002; Shao *et al.* 2002). The single measurement precision that we refer to is the precision obtained by combining multiple one dimensional relative delay measurements between the target star and multiple reference stars in a single visit (1 hour). In our simulations, we set $\sigma_{SIM} = 1\mu$as, but most of our results can be scaled to other values of σ_{SIM} using the "scaled signal",

$$S \equiv \frac{\alpha}{\sigma_{SIM}}, \tag{1}$$

where

$$\frac{\alpha}{''} \equiv \frac{m}{M} \frac{a}{\mathrm{AU}} \frac{\mathrm{pc}}{D}, \tag{2}$$

α is the semi-amplitude of the stars motion on the plane of the sky, m is the mass of the planet, M is the mass of the star, a is the semi-major axis of the planet, and D is the distance to the star. For example, a Jupiter mass planet (M_J) with a 3d, 1yr, or 5yr orbital period would result in $S = 3.9$,

96, or 280, assuming a 1 $M_\odot$ star at a distance of 10 pc. Similarly, a Neptune (Earth) mass planet orbiting a 1 $M_\odot$ star 10 pc away would induce a perturbation of magnitude $S = 0.21$, 5.1, or 15 (0.012, 0.30, or 0.88) for a 3d, 1yr, or 5yr orbital period.

Stars in wide binary systems will have an unknown acceleration in addition to the usual astrometric parameters (position, distance, and proper motion). The angular acceleration ($\vec{a}$) induced by a wide binary companion is

$$\frac{\vec{a}}{\mu \text{as yr}^{-2}} = 4\left(\frac{M_c}{M_\oplus}\right)\left(\frac{r}{1000\text{AU}}\right)^{-2}\left(\frac{D}{10\text{pc}}\right)^{-1}\cos i,$$

where M_c is the mass of the binary companion, r is the three dimensional separation between the primary and its companion, D is the distance between the target star and the Earth, and $\cos i$ is the cosine of the angle between the plane of the sky and the vector between the two stars. This can be easily obtained from Newton's laws by solving for the acceleration of a body due to due to a point mass (M_c) at distance (r), projecting onto the plane of the sky, and dividing by the distance to the star (D). We restrict our attention to wide binary companions for which the orbital period is much longer than the duration of the astrometric survey (the expected SIM mission lifetime is 5-10 years). Thus, the perturbations due to the binary companion can be accurately modeled as a constant acceleration of the target star.

Stars with multiple planetary mass companions will have an astrometric signal that is the superposition of the perturbations from each planet, implicitly depending on the gravitational perturbations between the planets. In this paper, we model the motion of each planet as a Keplerian orbit, even for systems with multiple planets. While gravitational interactions among the planets can result in significant deviations from purely Keplerian orbits (e.g., GJ 876), most of the planetary systems discovered by the radial velocity method can be well modeled by planets on non-interacting Keplerian orbits, at least for time scales comparable to the expected lifetime of SIM.

2.1. Model Planets and Observations

We simulate astrometric observations of many hypothetical stars. Each star is assigned a position (RA, Dec), distance (D), proper motion ($\vec{v_\perp}/D$), mass (M). The stellar positions are distributed uniformly in a shell of radius 10 parsecs centered on the Sun. The stellar velocities are drawn from a three-dimensional Gaussian distribution with mean 0 km s^{-1} and standard deviation 40 km s^{-1} in each direction. The stellar masses are set to $1M_\odot$ and the stellar velocities are randomly directed in space. When considering planets in wide binary systems in §3, we augment the model of Ford (2004) by assigning each star an angular acceleration ($\vec{a}$). Each star is also assigned one or two planets, depending on whether considering the effects of wide stellar binaries in §3 or multiple planet systems in §4.

As in Ford (2004), each planet is assigned a mass (m), orbital period (P), orbital eccentricity (e), inclination of the orbital plane to the plane of the sky (i), argument of pericenter (ω), longitude

of ascending node (Ω), and mean anomaly at a specified time (M_o). The masses and orbital periods of the simulated planets are drawn independently from the planetary mass and period function determined by Tabachnik & Tremaine (2002) and are based on radial velocity observations of massive planets. The planet masses range from one Earth mass ($1M_\oplus$) to ten Jupiter masses ($10M_{Jup}$) and the orbital periods range from 2 days to a maximum orbital period, $P_{\max} = 2P_{SD}$, twice the duration of the astrometric survey (P_{SD}). The eccentricities are drawn from a uniform distribution between 0 and 1. The orbits are drawn independently and randomly oriented in space. We consider both $P_{SD} = 5$ and 10 years, since there can be significant differences in the efficiency of detection for planets in the habitable zone depending on the duration of the survey (as we will show in §4). For two-planet systems, we have conducted additional simulations fixing the mass and/or orbital period of one or both planets to help visualize how the sensitivity depends on the other parameters.

2.2. Data Analysis

After simulating the observations, we attempt to fit a no-planet model that includes only the star's five astrometric parameters (D, RA, Dec, and the two components of $\vec{v}$) as in Ford (2004). In all our fitting we use use the Levenberg-Marquardt algorithm (Press *et al.* 1992) combined with good initial guesses of the parameters as described in Ford (2004). When considering the effects of planets in binary star systems in §3, we also allow the no-planet model to include an unknown acceleration. After identifying the best-fit astrometric parameters, we evaluate the appropriateness of the no-planet model by a χ^2 test using the usual sum of squares of the residuals for the no-planet model χ_0^2.

When considering the effects of planets in binary star systems, if the no-planet model (allowing for an unknown constant acceleration) can be rejected with 99.9% confidence, then we apply the Levenberg-Marquart algorithm to obtain the best-fit model with both a constant acceleration and one planet. When fitting for orbital parameters, we use use Thiele-Innes coordinates as described in Ford (2004). We calculate χ_1^2 for the new model (including both a constant acceleration and one planet) and detect the planet if χ_1^2 is significantly less than χ_0^2, according to an F-test.

When considering two-planet systems in §4 & 5, if a χ^2 test can reject the no-planet model with 99.9% confidence, then we proceed to fit two new models, each including only one of the two planets (labeled a & b). We calculate χ_{1a}^2 and χ_{1b}^2 for these two models and detect planet a (b) if χ_{1a}^2 (χ_{1b}^2) is significantly less than χ_0^2, according to an F-test. If both one-planet models can be rejected with 99.9% confidence by a χ^2 test, then we proceed to fit a two-planet model (including both planets a & b) and calculate χ_2^2. If χ_2^2 represents a significant improvement from both χ_{1a}^2 and χ_{1b}^2 according to an F-test, then we detect both both planets (a & b) simultaneously. Note that it is technically possible to detect both planets simultaneously but not individually (if χ_2^2 is significantly better than χ_0^2, even when neither χ_{1a}^2 nor χ_{1b}^2 are). It is also technically possible to detect both planets individually but not simultaneously (if both χ_{1a}^2 and χ_{1b}^2 are significantly better

than χ_0^2, but χ_2^2 is not). This can occur when the data provide evidence for at least one planet, the data still permit multiple very different orbital solutions, and the data do not yet provide sufficient evidence for two planets. In our subsequent discussion of two-planet systems, we consider planet a (b) to be detected if either χ_{1a}^2 (χ_{1a}^2) or χ_2^2 is significantly less than χ_0^2 according to an F-test. This criteria is slightly optimistic since it occasionally counts a planet as detected even when multiple qualitatively different orbital solutions are still viable models.

While Bayesian techniques have already been applied to orbit fitting (Ford 2005a) and model selection (Ford 2005b) for radial velocity planet surveys, all previous studies of SIM planet searches have relied on frequentist statistical methods. We recognize the superiority of a Bayesian approach and expect that future work will develop the algorithms necessary for Bayesian parameter estimation and model selection to be applied to the actual SIM planet searches. Here we employ frequentist methods due to computational limitations, since we must simulate orders of magnitude more systems than will actually be observed by SIM.

We repeat these calculations for millions of stars to determine the efficiency for detecting planets with in various binary star and multiple planet systems. It is important to note that, when finding best-fit models, we use only a local search algorithm, primarily due to the computational limitations when performing millions of orbital fits. We use parameters for both the star and planet typically accurate to 1%. Our results should be considered optimistic. In practice, it will be necessary to conduct a global search to provide initial guesses and it may be more difficult for a global search to find the best-fit model. This is a subject worthy of separate investigation. While Konacki, Maciejewski & Wolszczan (2002) provide one method of obtaining initial guesses, it has not been demonstrated to work for multiple planet systems or for systems with a modest signal-to-noise ratio.

3. Results for Planet in Binary Star Systems

We have simulated observations of many stars with a planet to determine our ability to detect planets and measure their masses and orbital parameters. To understand the effects of a wide binary companion, we compare the results of simulations in which we assume an unknown acceleration term with simulations in which we assume the acceleration is known. We also compare the results of simulations with various values for the magnitude of the acceleration, the planetary orbital period, the planetary eccentricity, and the magnitude of the scaled signal.

3.1. Rates versus Acceleration

First, we compare the overall rates for detecting and characterizing planets as a function of the projected angular acceleration, averaged over the distance to the star, planetary mass, planetary orbital period, and other parameters (e, ω, i, Ω, and M_0; see Fig. 1). The top pair of lines is for

detections, the middle pair of lines is for measuring the planetary mass with 30% accuracy, and the bottom pair of lines is for measuring the planetary orbital parameters with 10% accuracy. In each pair the top line is for stars with a known acceleration and the bottom line is for stars with an unknown acceleration. In each case, the unknown acceleration slightly reduces the overall rates for detecting and characterizing the planet, but the size of the effect is independent of the magnitude of the acceleration. Therefore, for the remainder of the paper, we set the actual acceleration term to zero, and compare the results obtained by assuming that the acceleration is known to be zero to the results when we consider the acceleration to be unknown and attempt to find the best-fit acceleration term.

3.2. Rates versus Scaled Signal

While Fig. 1 demonstrates that the overall rates for detecting and characterizing planets is only slightly affected by including an unknown constant acceleration, the effect can be much more significant for certain values of the scaled signal and planetary orbital period. In Fig. 2 we plot the rates for detecting and characterizing planets as a function of the scaled signal, both including (solid lines) and omitting (dotted lines) a constant acceleration term. In each row of panels, we restrict our attention to a small range of planetary orbital periods. The far-left column of panels is for detecting the planet, the center-left column is for measuring the mass with 30% accuracy, the center-right column is for measuring the mass with 10% accuracy, and the far-right column is for measuring the orbital parameters with 10% accuracy. We have extended the range of planetary orbital periods up to 10 years (twice the survey duration) for Figs. 2-4.

For small values of the scaled signal, the planet is not detected, regardless of the orbital period or the inclusion of an acceleration term. For sufficiently large values of the scaled signal, the planet can be detected and characterized even for orbital periods somewhat longer than the duration of the astrometric survey. However, for intermediate values of the scaled signal and periods comparable to the mission lifetime, there can be a significant reduction in the rates for detecting planets and measuring their orbits, when an unknown constant acceleration is included.

3.3. Rates versus Planetary Orbital Period

In Fig. 3 we plot the rates for detecting and characterizing planets as a function of the planetary orbital period. In each panel the solid line is for models including an unknown constant acceleration and the dotted line assumes no acceleration. In each row of panels we fix the value of the scaled signal. While there is little difference for planetary orbital periods less than 2.5 years (half the survey duration), the presence of a wide binary companion can dramatically lower the detection efficiency for longer planetary orbital periods. The narrow dips for small orbital periods are aliasing due to observing at nearly periodic intervals.

Since the scaled signal is influenced by both the planet mass and orbital period, we also consider the rates for detecting and characterizing planets as a function of the planetary orbital period, after dividing the population into subsets according to the mass of the planet (see Fig. 4) The rates for detecting giant planets and measuring their masses and orbital parameters will not be significantly affected by the presence of wide binary companions (since we expect most giant planets to cause a large scaled signal or be in a short-period orbit). However, detectable planets with masses less than $20 M_\oplus$ are expected to induce a modest scaled signal and/or to have orbital periods comparable to the duration of the astrometric survey. Thus, the rates for detecting terrestrial mass planets and measuring their orbits may be significantly reduced when it is necessary to allow for the acceleration of a wide binary companion.

3.4. Rates versus Planetary Orbital Eccentricity

Next, we investigate the effect of a binary companion on the rates for detecting planets and measuring their masses and orbital parameters as a function of the planetary orbital eccentricity (see Fig. 5). While the rates do have a weak dependence on the eccentricity, they are not significantly altered by allowing for an unknown constant acceleration term.

3.5. Rates versus Planetary Mass

Finally, we show the effect of a binary companion on the rates for detecting planets and measuring their masses and orbital parameters as a function of the planetary mass (see Fig. 6). In each row of panels we focus on planets with orbital periods in a given range (top: 1-3 yr, middle: 3-5 yr, bottom: 5-7 yr). While these calculations assumed a distance of 10pc and 24 pairs of 1-d observations with single measurement precision of 1μas, the results can be scaled to other distances and measurement precisions. For orbital periods much shorter than the duration of the astrometric survey, there is little effect due to the unknown acceleration term. However, the rates of detecting planets and measuring their orbital parameters can be significantly affected for low mass planets when the orbital period approaches or exceeds the duration of the survey.

4. Results for Planets in Multiple Planet Systems

In this section, we present the results of simulated observations of many stars with two planets to determine our ability to detect planets and measure their masses and orbital parameters. To understand the effects of multiple planets, we compare the results with simulations including only a single planet.

We tabulate some of our results in Table 1 (electronic version only). The table includes a

subset of our results particularly relevant to one of the questions that we address in this section. We list the mass and orbital period of each planet (named A and B) in the first four columns. In columns 5 and 6 we list the probabilities of detecting planet A or B, if it were the only planet in the system. In columns 7 and 8 we list the efficiencies of detecting planets A and B in a two-planet system with parameters given in columns 1-4. We define the efficiency for detecting a planet to be the probability of detecting the planet when in the two-planet system divided by the probability of detecting the planet if it were the only planet in the system. In column 9 we list the probability of detecting both planets simultaneously.

In Figure 7 we show the probability contours for detecting a single planet as a function of its orbital period and the scaled signal, averaging over the mass and other parameters. The dotted lines are for rejecting the best-fit no-planet model with 99.9% probability, while the solid lines also require that the reduction in χ^2 due to using the best-fit one-planet model is significant at the 99.9% level. Note that this paper requires a planet to pass the latter test to be considered detected and that this is a more strict requirement than was used by Sozzetti *et al.* (2002) and Ford & Tremaine (2003). The sharp rise in required signal near $P = 5$ yr is due to the duration of the simulated astrometric survey.

In Figure 8 we show probability contours for detecting planets in a two-planet system as a function of their scaled signals, averaging over their masses, orbital periods (up to 5 years), and other parameters. The solid lines are for detecting both planets, and the dashed line and dotted-dashed line are for detecting either planet (regardless of whether the other planet is detected). For reference, the dotted lines show the probability contours for detecting a single planet, if the other planet were not present. The bold contours are for a 50% probability of detection. When one planet has a small scaled signal ($S \leq 1$), it has only a slight effect on the efficiency for detecting the other planet. However, when one planet has a significant scaled signal ($S \geq 4$), then the scaled signal necessary to detect the other planet is significantly increased (by a factor ~ 2.5).

Next, we consider several questions about how the planet finding capabilities of SIM will be affected by the presence of two planets in light of our simulations. While our numerical simulations cover a wide range of parameter space, it is difficult to visualize our results over the full multi-dimensional parameter space. Therefore, the discussion of our results concentrates on the most important factors, the planet masses and orbital periods. We focus on the effects of additional giant planets ($\sim 1 M_J$) and low mass planets ($\leq 20 M_\oplus$) with orbital periods in one of three categories, short (~ 3d), intermediate ($\sim 1 - 3$yr), or long (~ 12yr).

4.1. Is a giant planet harder to detect when a long-period planet in present?

First, we consider systems with one giant planet in a $1 - 3$yr orbit and an additional planet with a 12 year orbital period. The inner giant planet is easily detectable in the absence of the outer planet, and the efficiency is only slightly affected by the presence of a distant outer companion.

In Figure 9 we plot the probability of detecting a planet with a 1 year orbital period as a function of the mass of that planet, m_1. The solid line is for a single planet, while the other lines are for a two-planet system with a second planet of various masses in a 12 year orbit. The main effect of the outer planet is to raise the mass of the smallest detectable inner planet by a factor of ~ 3.

In Figure 10 we plot the probability of detecting an inner planet as a function of the planet's orbital period, P_1. The solid lines are for the planet by itself, and the dotted lines are for the inner planet when there is a second planet in a long-period orbit ($P_2 = 12$ yr). The different rows of panels are for detecting a planet of different masses, and the different columns of panels are for different masses of the outer planet. For an inner planet with mass $1M_J$ (top), the efficiency is only slightly reduced for orbital periods less than the mission duration in the presence of an outer planet. (In the top panels, the solid line is very near 1 for all periods.)

4.2.   Is a giant planet harder to detect when a short-period planet is present?

Next, we consider systems with one giant planet in a $1 - 3$yr orbit and an additional planet with a 3 day orbital period. The outer planet is easily detectable in the absence of the inner planet, but the probability of detecting the outer planet is slightly reduced ($\sim 10\%$) due to the presence of the inner planet.

In Figure 11 we plot the probability of detecting a planet in a 1 year orbit as a function of the mass of a second planet, m_2 in a short-period orbit, $P_2 = 3$ d. The horizontal lines show the probability of detecting the outer planet in the absence of the inner planet for reference. The solid and dotted lines (top) are for an outer planet with mass $m_1 = 1M_J$ and the short and long-dashed lines (bottom) are for an outer planet of mass $m_1 = 20M_\oplus$. The probability of detecting the outer planet is somewhat reduced, even for a $1M_J$ mass outer planet in the presence of a low-mass planet in a 3 day orbit. The probability of detecting a $20M_\oplus$ outer planet is dramatically reduced by the presence of a short-period planet with mass $m_2 \geq 0.3M_J$. As we discuss in §5, adding a modest number of radial velocity observations can often restore the sensitivity for detecting such planets.

In Figure 12 we plot the probability of detecting an outer planet as a function of the planet's orbital period, P_1. The solid lines are for the planet by itself, and the dotted lines are for an outer planet when there is a second planet in a short-period orbit ($P_2 = 3$ d). The different rows of panels are for detecting a planet of different masses, and the different columns of panels are for different masses of the inner planet. For an outer planet with mass $1M_J$ (top), the efficiency is only somewhat reduced ($\sim 20\%$) when in the presence of an inner planet.

4.3. Is a giant planet harder to detect when another giant planet is nearby?

We now consider systems with two giant planets with roughly comparable orbital periods (e.g., 1 and 3 years). These planets would be easily detectable in isolation and are only slightly affected by the presence of a nearby giant planet. This is the type of two-planet system for which it is most likely that SIM will be able to detect both planets.

In Figure 13 we plot the probability of detecting a planet (1) in a 1 year orbit as a function of the mass of a second planet, m_2 in a 3 year orbit. For reference, the horizontal lines are for the inner planet in isolation. The top pair of lines is for $m_1 = 1M_J$, and the bottom pair of lines is for $m_1 = 20M_\oplus$. A $1M_J$ inner planet (top) is only slightly affected, but a 20 $M_\oplus$ inner planet (bottom) can become dramatically more difficult to detect when $m_2 \geq 10M_\oplus$. As we discuss in §5, adding radial velocity observations can often restore the sensitivity for detecting such planets.

In Figure 14 we plot the probability of detecting a planet as a function of its orbital period, P_1. The solid lines are for a single planet, while the dotted lines are for a two-planet system with a second planet in a 3 year orbit. The different rows of panels are for detecting an inner planet of different masses and the different columns are for different mass of the outer planet. The probability of detecting a $1M_J$ planet (top left) can be somewhat affected for some orbital periods, but it is only slightly affected for orbital periods between ~ 0.5 and 5 years, where SIM will be most sensitive.

4.4. Is a giant planet harder to detect when low-mass planet is nearby?

It is similar for systems with one giant planet and one low-mass planet with roughly comparable orbital periods (e.g., 1 and 3 years). The giant planet is still easily detectable for most orbital periods, and there is even a reasonable chance of detecting the lower mass planet for some masses and orbital periods. There is only a small decrease in efficiency for orbital periods near the orbital period of the low-mass planet (see Figure 13, top center and top right).

4.5. Is a low-mass planet harder to detect when a long-period planet is present?

The probability of detecting a low-mass planet is significantly reduced in the presence of a long-period outer planet. For an inner planet with mass $20M_\oplus$, there is a significant reduction in the efficiency across the entire range of orbital periods that SIM will probe (see Fig. 10, bottom). In particular, a $1M_J$ mass planet with a 12 year orbital period drastically reduces the probability of detecting a $20M_\oplus$ mass planet with a $2-5$ year orbital period from close to 100% to $20-60\%$.

4.6. Is a low-mass planet harder to detect when a short-period planet is present?

The probability of detecting a low-mass planet can also be reduced due to the presence of a short-period inner planet. The effect is somewhat significant ($\sim 10\%$) for low-mass short-period planets, and it becomes extremely difficult to detect an outer planet with mass $20M_\oplus$ for a sufficiently massive short-period planet (see Fig. 11, short-dashed curve). For example, the presence of a $1M_J$ inner planet reduces the probability of detecting a $20M_\oplus$ planet with an orbital period near 5 years by $\sim 25\%$ and by even more for shorter orbital periods (see Fig. 2, bottom left). On the other hand, the presence of a $20M_\oplus$ planet in a short-period orbit, results in only a $\sim 15\%$ reduction in the probability of detecting a $20M_\oplus$ planet with orbital period $\sim 1 - 5\mathrm{yr}$ (see Fig. 6, bottom right). Fortunately, the addition of radial velocity observations can significantly improve the probability of detecting the low-mass planet, as discussed in §5.

4.7. Is a low-mass planet harder to detect when a giant planet is nearby?

The probability of detecting a low-mass planet can also be reduced due to the presence of a nearby giant planet. For example, detecting a $20M_\oplus$ planet in a 1 year orbital period is very unlikely in the presence of a planet with mass $\geq 6M_\oplus$ with a 3 year orbital period (see Fig. 13, dashed curves). This causes a decrease in efficiency by $\geq 50\%$ over the entire range of orbital periods that SIM will probe (see Fig. 14, bottom left). Again, the addition of radial velocity observations can significantly improve the probability of detecting the low-mass planet (see §5).

4.8. Is a low-mass planet harder to detect if another low-mass planet is nearby?

The presence of two nearby low-mass planets also reduces the probability of detecting either planet. For example, for two $20M_\oplus$ planets with orbital periods of 1 and 3 year, there is a $\geq 50\%$ reduction in the probability to detect either planet (see Fig. 14, bottom center). For a pair of planets with masses $20M_\oplus$ and $1 - 5M_\oplus$, the effect is smaller and only occurs for a portion of the orbital periods that SIM will probe (see Fig. 14, bottom right).

5. Adding Radial Velocity Observations

Combining an astrometric planet search with radial velocity observations can result in an increased sensitivity to low mass planets (Eisner & Kulkarni 2002). Just as we defined S as the scaled signal for astrometric observations, we can define

$$R = \frac{m}{M} \frac{2\pi a}{P} \frac{\sin i}{\sigma_{RV}}, \tag{3}$$

where σ_{RV} is the single measurement precision for a radial velocity observation. When $R \gg S$, radial velocity observations are typically more efficient at detecting a planet and measuring the five orbital parameters accessible from radial velocities alone (except for a small fraction of orbits with pathological orientations). When $S \gg R$, astrometric observations are more efficient for detecting a planet and measuring it's mass and orbital parameters. The transition between these two regimes is independent of the star and planet masses and occurs at an orbital period

$$P_t = 0.30\mathrm{yr}\sin i \left(\frac{D}{10\mathrm{pc}}\right)\left(\frac{\sigma_{SIM}}{1\mu\mathrm{as}}\right)\left(\frac{\mathrm{m/s}}{\sigma_{RV}}\right). \tag{4}$$

Eisner & Kulkarni (2002) found that combining astrometric and radial velocity observations for a single planet near this transition region results in an improvement in sensitivity comparable to that which is expected by simple scaling laws. A simplistic analysis might suggest that combining astrometric and radial velocity observations will provide a significant improvement only for a relatively small fraction of planets with orbital periods near this transition region ($0.5P_t \leq P \leq 2P_t$), and that radial velocity observations are of relatively little value for searching the habitable zones of nearby stars (Shao $et\ al.$ 2002). However, this argument does not apply to multiple planet systems.

Radial velocity surveys have shown that a star with one giant planet within $\sim 3\mathrm{AU}$ is more likely to have a second giant planet within $\sim 3\mathrm{AU}$ than a randomly chosen star of similar metallicity and spectral type (Fischer $et\ al.$ 2001). Based on the currently known radial velocity planets, at least $\sim 13\%$ of planetary systems have multiple planets and $\sim 26\%$ of known planets are in a multiple planet system. Since additional planets may be found orbiting stars with a only single currently known planet, these fractions are likely to increase as additional planets are discovered by either radial velocity or astrometric planet searches. For planets in multiple planet systems, the combination of astrometric and radial velocity observations could be particularly valuable, as one planet may be easier to detect with radial velocity observations and another planet may be easier to detect with astrometric observations. For example, many of the currently known multiple planet systems have one giant planet in a short-period orbit and a second more distant giant planet. For such systems, radial velocity measurements can easily constrain five of the seven orbital parameters for the inner giant planet, allowing the astrometric observations to more easily detect a more distant planet.

We have performed additional simulations to quantify the improvement obtained from adding radial velocity observations to a SIM planet search. Our methods closely follow those described in §2, but we add 12, 24, or 48 radial velocity observations at random times during the astrometric survey. We also include a Gaussian noise source with standard deviation, $\sigma_{RV} = 3\mathrm{m/s}$, the single measurement precision for radial velocity observations. Current radial velocity searches have demonstrated a measurement precision of $\simeq 1\mathrm{m/s}$, but stellar rotation and activity typically set the effective precision for measuring the gravitational perturbation due to planetary companions near $\simeq 1-5\mathrm{m/s}$, even for inactive stars (Wright 2005). The orbital fitting is done as before, fitting the orbits of both planets to the astrometric and radial velocity observations simultaneously. As for our simulations of purely astrometric surveys, we require that the reduction in χ^2 be significant

according to an F-test for a planet to be detected. Note that since we are interested in systems with multiple planets, methods based on the areal constant are not applicable (Pourbaix 2002).

First, we present our results for systems with one planet in a 1 year (left) or 3 year (right) orbit and an additional giant planet in a short-period orbit (3 days). In Fig. 15 we show the probability of detecting the more distant planet as a function of its mass (regardless of whether the short-period planet is detected). The inner planet has a mass of $1M_J$ (top) or $20M_\oplus$ (bottom). The solid line style shows the probability of detecting the more distant planet for a survey with no radial velocity observations, while the other line styles show the improvement from adding 12 (dotted), 24 (dotted-dashed), or 48 (dashed) radial velocity observations. Without the radial velocity observations, the presence of a short-period giant planet (top panels) would significantly reduce SIM's sensitivity to additional low-mass planets. However, even a modest number of radial velocity observations can fully compensate for the additional complexity of a two-planet model. For a $20M_\oplus$ short-period planet (bottom panels), the effects are less significant.

Next, we present our results for such two-planet systems as a function of the mass of the short-period planet (See Fig. 16). We show results for simulations where the more distant planet has a mass of $0.3M_J$ (top panels), $20M_\oplus$ (upper middle panels), $10M_\oplus$ (lower middle panels), and $5M_\oplus$ (bottom panels). The columns and line styles are the same as for Fig. 15. When the short-period planet has a sufficiently small mass, even radial velocity observations have difficulty constraining its orbit, so the radial velocity observations can provide only a modest improvement in the probability of detecting the more distant planet. When the short-period planet is sufficiently massive, adding radial velocity observations can dramatically improve the probability of detecting a more distant planet. This effect is particularly impressive for relatively low-mass planets ($\sim 5 - 50M_\oplus$ at 10pc) which are a prime target for the SIM planet searches. The dip in the curves at intermediate masses occurs when the perturbations from the two planets are comparable, making it more difficult to separate the two signals.

6.   Discussion

6.1.   Wide Binary Stars

When we allow the no-planet model to include an unknown constant acceleration term appropriate for a wide binary companion, the sensitivity of our simulated astrometric surveys is unaffected for planets with orbital periods much shorter than the duration of the survey, but the sensitivity is significantly decreased for orbital periods approaching the duration of the survey. For planets with orbital periods longer than the duration of the survey, the reduced sensitivity due to an unknown acceleration can be much larger. While the unknown acceleration due to a distant binary companion will decrease the rate at which very low mass planets are detected, the efficiency for detecting giant planets around nearby stars will be only slightly reduced, since these either have a short orbital period (small semi-major axes) or a large signal (large semi-major axis).

These results have important consequences for choosing targets for an astrometric planet search such as those planned for SIM. If the primary purpose of a 5 yr survey were to detect low mass planets with orbital periods less than 3 yr, then it would be advantageous to target nearby wide binary stars rather than more distant single stars. This would be particularly relevant if searching for planets in the habitable zone of a solar-type star. On the other hand, if searching for low mass planets with orbital periods slightly less than the survey duration, then the presence of a wide binary companion is likely to significantly reduce the sensitivity. This could be particularly relevant if searching for a terrestrial mass planet near the habitable zone of an A or F star, as suggested by Gould, Ford, & Fischer (2003). If the SIM mission were extended to ten years, then the unknown acceleration due to a wide binary companion would not cause a significant reduction in sensitivity when searching for planets in the habitable zones of nearby stars, regardless of spectral type.

6.2. Two-Planet Systems

When planning the SIM planet searches, it will also be important to consider the effects of multiple planet systems. We have presented results of simulated observations for a wide variety of two-planet systems. First, we make some limited comparisons to the results of Sozzetti *et al.* (2003). Sozzetti *et al.* (2003) claim that the sensitivity for multiple planet systems with scaled signal $S \sim 1$ is not significantly reduced compared to single planet systems, but they tolerate an increased false alarm rate (of up to 10%). We hold the false alarm rate fixed (at 0.1%), and find that then the scaled signal required to detect a planet increases when there are multiple planets. While this makes detailed comparisons difficult, it illustrates an important capability of the SIM mission. While solid detections (e.g., low false alarm probability, $\sim 0.1\%$) are an important goal of the SIM planet searches, there is also significant value in the inevitable marginal detections (e.g., false alarm probability, $\sim 50\%$). These marginal detections can provide an enriched sample of target stars for future direct imaging planet searches, such as TPF-C and TPF-I (Marcy *et al.* 2005). Additionally, tentative estimates of orbital parameters could be useful for maximizing the value of such observations. For example, many planets in the habitable zone will only be visible for a modest fraction of their orbit when they are near maximum separation from their star, as viewed from the Earth. Being able to time observations so as to avoid times when a planet is too close to the star for direct imaging, would save valuable observing time, allowing a greater number of stars to be searched more thoroughly. Similarly, preliminary estimates of a planet's orbital geometry could be used to choose telescope orientations which maximize their chance of imaging the planet and eliminate the need to take multiple images at various roll angles. Such synergies between SIM and direct imaging planet searches are an intuitive example of the value of the more general and rigorous framework provided by Bayesian adaptive experimental design that has previously been described in the context of radial velocity surveys (Ford 2005b) and purely astrometric surveys (Loredo 2004). We leave a more thorough investigation of the value of marginal detections and synergies between various detection techniques for future study.

Our simulations show that the probability that SIM will detect a planet is typically reduced when a second planet is present. For giant planets with orbital periods which SIM will probe, this is only a small effect for most masses and orbital periods (up to the mission duration) of the second planet. The probability of SIM detecting a low-mass planet is likely to be more significantly affected by an additional planet. While there is a high probability that SIM will detect single planets with masses $\leq 20 M_\oplus$ and orbital periods $0.5 \leq P \leq 5$ years, the probability can be significantly reduced by a second planet in a wide variety of locations. A giant second planet can significantly reduce the probability of detecting a low-mass planet, regardless of whether the giant planet has an orbital period of 3 days, 1 year, or 12 years. Fortunately, adding a radial velocity observations can dramatically improve SIM's sensitivity to low-mass planets in multiple planet systems.

For a purely astrometric survey, a no-planet model can be rejected 50% of the time when any planet causes a scaled signal of $S \geq 2.2$ (Sozzetti *et al.* 2001; Ford & Tremaine 2003). When a single planet causes a scaled signal $S \geq 4.6$, the masses and orbital parameters are measured sufficiently accurately that the best-fit one planet model significantly reduces χ^2 (compared to the best-fit no-planet model) 50% of the time (Ford & Tremaine 2003). However, if there is a second planet in the system, then a one-planet model often does not result in a significant improvement in χ^2 unless one planet causes a scaled signal of $S \geq 12$. When the planet inducing the smaller perturbation causes a scaled signal $S_< \leq 4$, it may be possible to detect the planet inducing the larger scaled signal for $4.6 \leq S_> \leq 12$. To obtain a two-planet model which significantly reduces χ^2 (compared to the best-fit one-planet model) 50% of the time, both planets need to cause a scaled signal $S \geq 12$ (See Fig. 2). When a radial velocity observations are added, the sensitivity of the combined survey becomes a function of the scaled signals and the orbital periods of both planets, making it difficult to summarize the results in a single figure. We have included figures that illustrate the sensitivity of combined surveys for several cases of particular interest (see Figs. 15 & 16). We find that such surveys are much more sensitive to low-mass planets (by a factor ~ 2–3 in mass) when there is an additional giant planet, particularly when the giant planet is in a short-period orbit. Thus, the combined astrometric and radial velocity survey typically has a sensitivity to low-mass planets in two-planet systems that is comparable to sensitivity to single low-mass planets for the astrometric survey alone.

6.3. Hierarchical and Many-Planet Systems

In this paper we have simulated systems with just three massive bodies (one star and two planets or two stars and one planet), and the large parameter space already makes a thorough study impractical. Therefore, we have not attempted to carry out simulations for four or more massive bodies, despite the fact that a few such planetary systems have already been discovered. Nevertheless, we can make some general comments about the challenges that such systems will create. Searching for planets around one star in a hierarchical triple (or higher multiple) star system should be very similar to searching for planets around one star in a wide binary system.

Long term stability of the planet requires that all stellar companions must be much farther away, so all such stars will move only slightly over the duration of observations. Therefore, the perturbation of the additional stars can be modeled as a single constant acceleration, and our simulations of wide binary stars should be directly applicable..

For planetary systems with two planets and a wide binary companion, we expect that the unknown acceleration due to the distant stellar companion will only be significant when at least one planets has an orbital period greater than half the mission duration. For such systems, the unknown acceleration will make it more difficult to detect and characterize the orbit of the outer planet. If the outer planet induces a perturbation comparable to or larger than the perturbation due to the inner planet, then it will also be more difficult to detect and characterize the orbit of the inner planet. In cases where the outer planet induces a perturbation small relative to that of the inner planet, the detection and characterization of the inner planet's orbit should be relatively robust to the unknown acceleration.

For planetary systems with three or more planets, the situation is more complicated. A comprehensive study of all plausible configurations is not feasible due to the enormous range of parameter space. Even a question-based approach similar to §4 would require an unreasonably lengthy text. Here we only raise a few qualitative concerns. Based on our experience analyzing radial velocity and simulated astrometric data sets, it is essential for the number of observations to be at least several times the number of free model parameters. For example, the radial velocity of a star orbited by three planets on Keplerian orbits is described 16 model parameters, yet the discovery papers announcing three planet systems were based on a much larger number of observations, 137 observations for υ And, 146 for 55 Cnc, 76 for HD 160691, 52 for HD 37124 (for which two qualitatively different orbital solutions were offered), and 155 for GJ 876. To model the astrometric motion of a star orbited by three planets requires 26 model parameters (2 position, 1 parallax, 2 velocity, 3 masses, and 3 sets of 6 Keplerian elements). Therefore, we expect that it will be extremely difficult to detect and accurately measure orbital parameters for three planet systems using only the currently planned SIM observations of 50-100 one dimensional observations per star over a five year mission. Allocating additional follow up observations during the first five years and/or extending the mission lifetime to ten years would be extremely valuable for characterizing such multiple planet systems. For multiple planet systems where at least one planet has an orbital period less than P_t, radial velocity observations could significantly improve the ability of SIM to detect and measure the orbital parameters of additional planets at larger distances, by accurately measuring the orbits of the short-period planets.

6.4. Consequences for SIM

Our results have significant consequences for the SIM planet searches. On the positive side, SIM will often be able to detect and measure the astrometric parameters of both planets in systems with two giant planets with orbital periods 60 d$\leq P \leq$ 5 yr. However, if most low-mass planets are

typically in systems with multiple planets, then SIM along would have more difficulty detecting the low-mass planets in these systems without accompanying radial velocity observations. As discussed in §5, the addition of a modest number of high precision radial velocity observations can significantly increase the survey's sensitivity for various types of planetary systems. This implies that it is very important that the SIM planet search be accompanied by radial velocity observations whenever possible (e.g., even for M stars that require long exposure times for precise radial velocities). While such observations are already underway for many SIM planet search target stars, for other stars (e.g., F & A stars) it is more difficult to obtain precise radial velocities (e.g., due to increased activity and rotational broadening of spectral lines). When interpreting the results of the SIM planet searches, it will be important to consider the variation in SIM's sensitivity to low-mass planets in multiple planet systems as a function of the quality of radial velocity constraints.

If the mission lifetime of SIM were extended to 10 years, then the sensitivity to low-mass planets is further improved. However, the improvement due to adding radial velocity information is reduced (see Figs. 15 & 16, red curves for 10 year surveys in electronic version only). Even if the baseline mission lifetime were extended to 10 years, we believe it would still be important to obtain at least a modest number of radial velocity observations ($\sim 12-24$), so that low-mass planets can be identified early during the SIM mission, permitting additional astrometric measurements to be obtained for these particularly interesting system. It is important to remember that the probabilities presented in this paper are for detection only. Additional observations will be necessary to precisely determine the various orbital parameters, which are of particular interest for multiple planet systems. If such systems can be identified early in the SIM mission, then it will be possible to allocate additional observations that can significantly improve the measurement of orbital parameters (e.g., Loredo 2004; Ford 2005b).

6.5. Review of Key Assumptions

It is important to keep in mind the assumptions and limitations of our simulations. The tables and figures presented assume a star 10pc away is observed with 24 pairs of 1-d astrometric observations with single measurement precision $\sigma_{SIM} = 1\mu$as, as suggested by the SIM planet search proposals (Marcy *et al.* 2002; Shao *et al.* 2002). While changing any of these parameters would affect the masses of planets which SIM is likely to detect, we believe our simulations provide valuable insight into how the presence of additional companions may affect SIM's sensitivity. For example, 88 of the stars selected as SIM narrow angle planet target are closer than 10pc, and 47 are closer than 6pc. For these targets, our results showing the sensitivity of SIM as a function of masses can be easily rescaled for the appropriate distances. Similarly, should the final performance of SIM differ from the specifications, our results can be rescaled for alternative values of the single measurement precision. In one sense our simulations are optimistic, since we assume that good initial estimates of the astrometric and orbital parameters are available for a local search algorithm. In practice, it will be necessary to generate initial guesses for these parameters from the observations themselves. We

believe that it is important for future studies to develop such algorithms, particularly for multiple planet systems. One reason our simulations might underestimate the sensitivity of SIM is due to the assumption of a non-adaptive scheduling algorithm. Early studies of adaptive scheduling algorithms for radial velocity searches suggest that adaptive scheduling could increase their sensitivity by a factor ~ 2 (Ford 2005b; Loredo 2004). While we believe it that such adaptive scheduling algorithms will be essential to maximize the value of SIM observing time, evaluating such algorithms is well beyond the scope of this study.

REFERENCES

Butler, R.P., Marcy, G.W., Vogt, S.S., Tinney, C.G., Jones, H.R.A., McCarthy, C., Penny, A.J., Apps, K., Carter, B.D. 2002, ApJ, 578, 565.

Eggenberger, A., Udry, S., Mayor, M. 2004 A&A 417, 353.

Eisner, J.A. & Kulkarni, S.R. 2001, ApJ, 550, 871

Eisner, J.A. & Kulkarni, S.R. 2001, ApJ, 561, 1107

Eisner, J.A. & Kulkarni, S.R. 2002, ApJ, 574, 426.

Faber, J.A., Rasio, F.A. & Willems, B. 2004, Icarus, 175, 248.

Fischer, D.A., Marcy, G.W., Butler, P.R., Vogt, S.S., Frink, S., & Apps, K. 2001 , ApJ, 551, 1107

Ford, E.B. & Tremaine, S. 2003 PASP, 115, 1171.

Ford, E.B. 2004, PASP, 116, 1083.

Ford, E.B. 2005a, AJ, 129, 1706.

Ford, E.B. 2005b, submitted to AJ (astro-ph/0412703)

Ford, E.B., Lystad, V., Rasio, F.A. 2005 Nature, 434, 873.

Lattanzi, M.G., Spagna, A., Sozzetti, A., Casertano, S. 2000, MNRAS, 317, 211.

Lee, M.H., Peale, S.J. 2002 ApJ 567, 596.

Loredo, T.J. 2004, in "Bayesian Inference And Maximum Entropy Methods In Science And Engineering: 23rd International Workshop" ed. G. J. Erickson and Y. Zhai; AIP Conference Proceedings 707, 330.

Marcy, G. et al. 2002 Discovery of Planetary Systems with SIM proposal, http://planetquest.jpl.nasa.gov/SIM/science_marcy.pdf

Marcy, G.W., Fischer, D.A., McCarthy, C., Ford, E.B. 2005 to appear in "Astronometry in the Age of the Next Generation of Large Telescopes" ed. P.K. Seidelmann & A.K.B. Money; ASP Conference Proceedings.

Press, W. H., Teukolsky, S. A., Vetterling, W. T., & Flannery, B. P. 1992, *Numerical Recipies in C: the Art of Sientific Computing.* New York: Cambridge University Press.

Robinson, J.P. & Bernstein, A.J. 1967, *IEEE Transactions on Information Theory,* IT-13.

Pourbaix, D. 2002, A&A 385, 686.

Shao, M. et al. 2002 Extrasolar Planet Interferometric Survey proposal, http://planetquest.jpl.nasa.gov/SIM/science_shao.pdf

Sozzetti, A., Casertano, S., Lattanzi, M.G., Spagna, A. 2001, A&A 373, 21.

Sozzetti, A., Casertano, S., Brown, R.A., Lattanzi, M.G. 2002, PASP, 114, 117.

Sozzetti, A., Casertano, S., Brown, R.A., Lattanzi, M.G. 2003, PASP, 116, 1072.

Sozzetti, A. 2005, PASP, 117, 1021.

Tabachnik, S. & Tremaine, S. 2002, MNRAS, 335, 151.

Takeda, G. & Rasio, F.A. 2005, ApJ, 627, 1001.

Wright, J.T. 2005 PASP 117, 657.
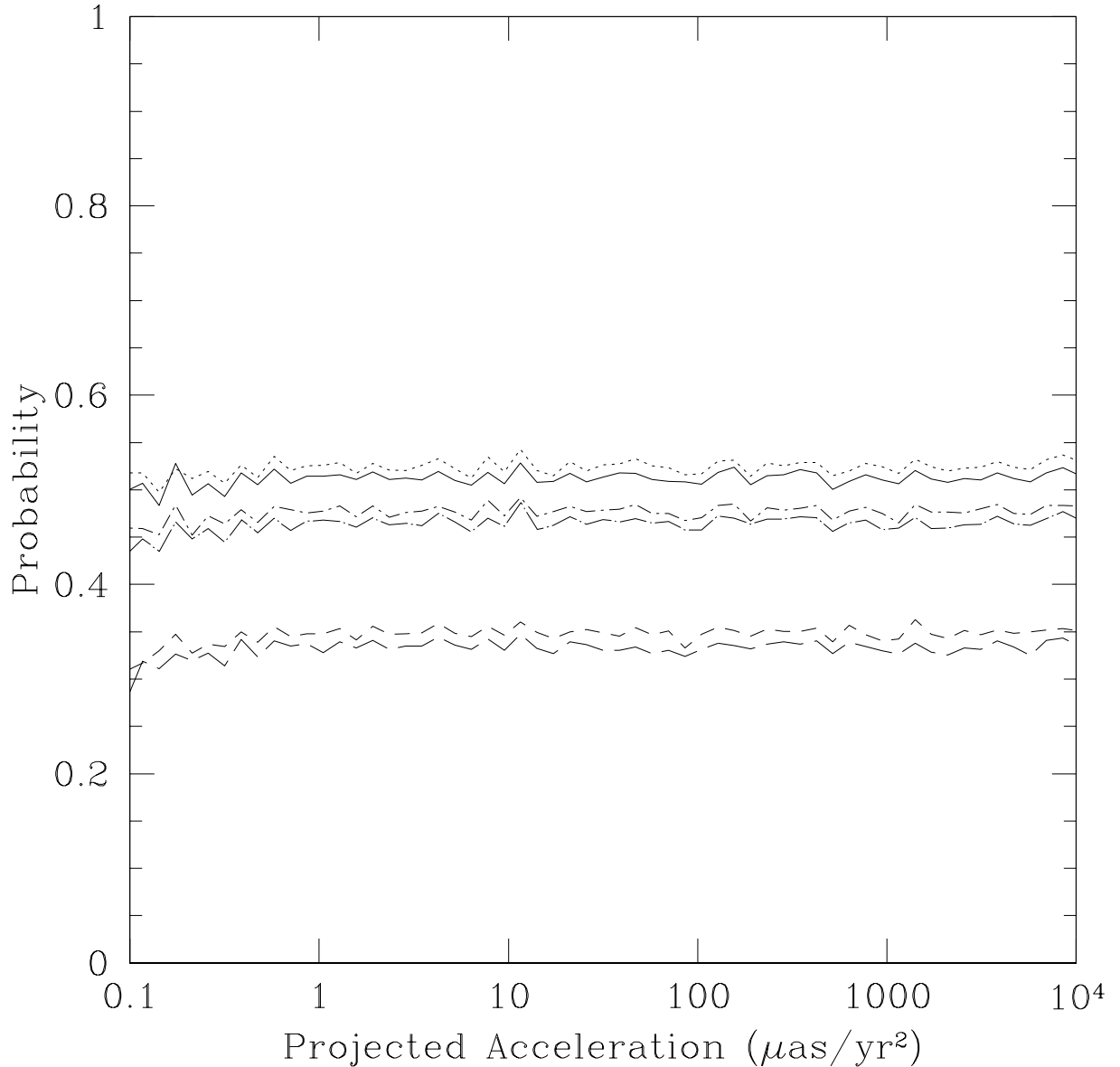
Fig. 1.— Here we compare the overall rates for detecting and characterizing planets as a function of the projected angular acceleration, averaged over the distance to the star, planetary mass, planetary orbital period, and other parameters. The top pair of lines is for detections, the middle pair of lines is for measuring the planetary mass with 30% accuracy, and the bottom pair of lines is for measuring the planetary orbital parameters with 10% accuracy. In each pair the top line is for stars with a known acceleration and the bottom line is for stars with an unknown acceleration. The additional acceleration has a negligible effect on the overall efficiency.
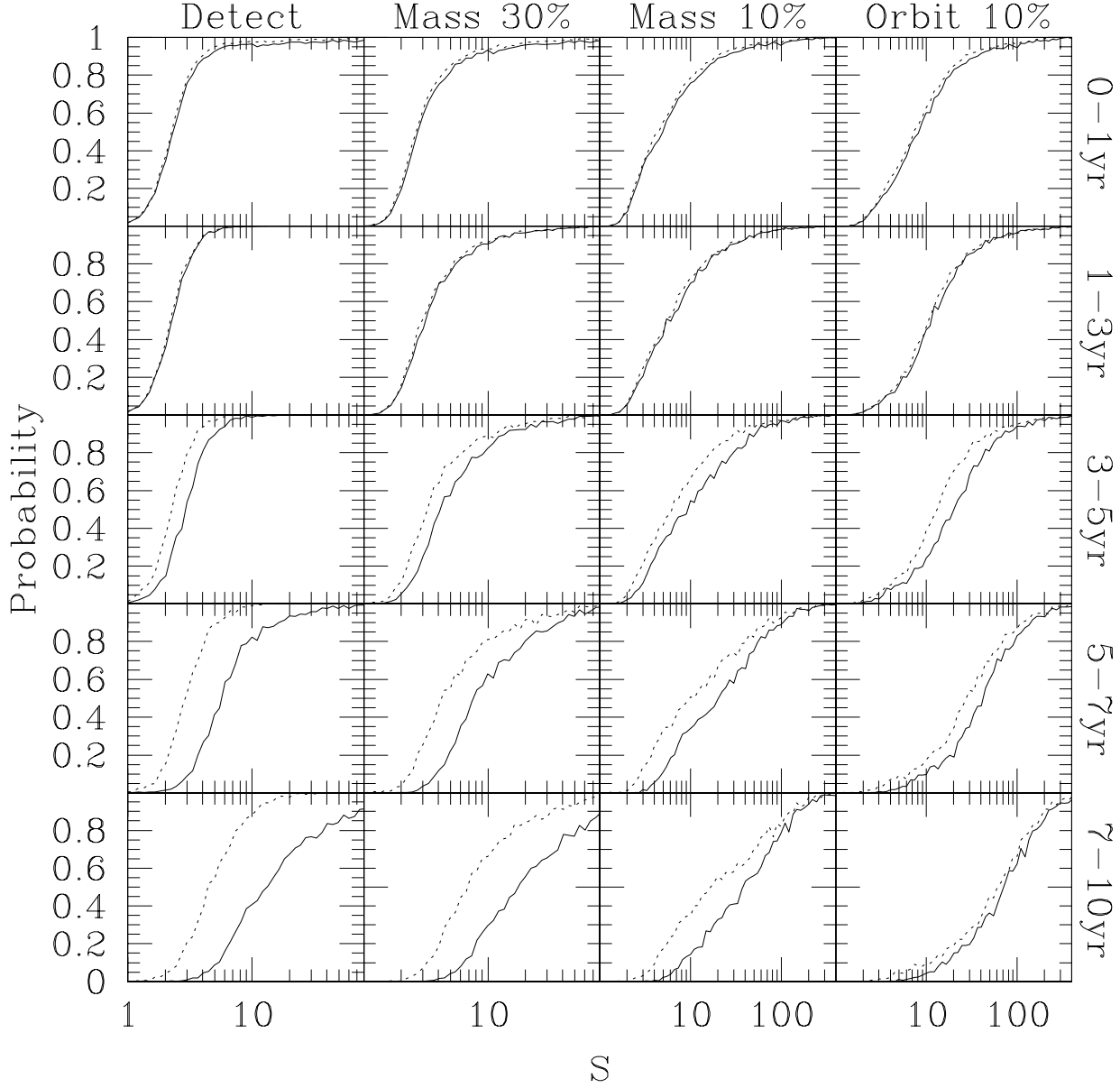
Fig. 2.— Here we plot the rates for detecting and characterizing planets as a function of the scaled signal, both including (solid lines) and omitting (dotted lines) a constant acceleration term. Each row of panels is for a different range of planetary orbital periods (top row: 0-1 yr, second row: 1-3 yr, middle row: 3-5 yr, fourth row: 5-7 yr, bottom row: 7-10 yr). The mission duration is assumed to be 5 yr. The far-left column of panels is for detecting the planet, the center-left column is for measuring the mass with 30% accuracy, the center-right column is for measuring the mass with 10% accuracy, and the far-right column is for measuring the orbital parameters with 10% accuracy.
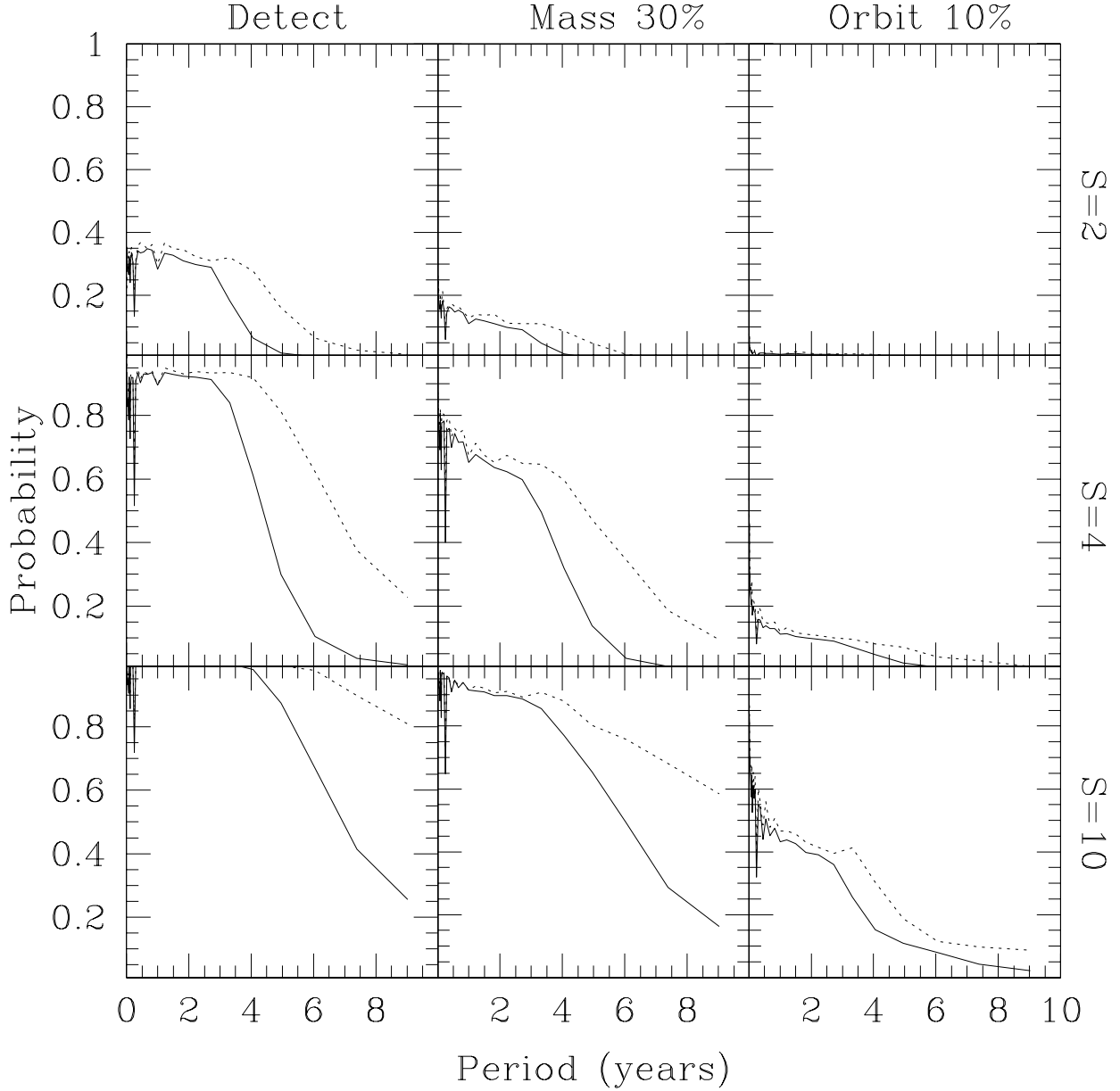
Fig. 3.— Here we show the rates for detecting and characterizing planets as a function of the planetary orbital period. In each panel the solid line is for models including an unknown constant acceleration and the dotted line assumes no acceleration. Each row of panels is for a different fixed value of the scaled signal (top: $S = 2$, middle: $S = 4$, bottom: $S = 10$). The left column of panels is for detecting the planet, the center column is for measuring the mass with 30% accuracy, and the right column is for measuring the orbital parameters with 10% accuracy.
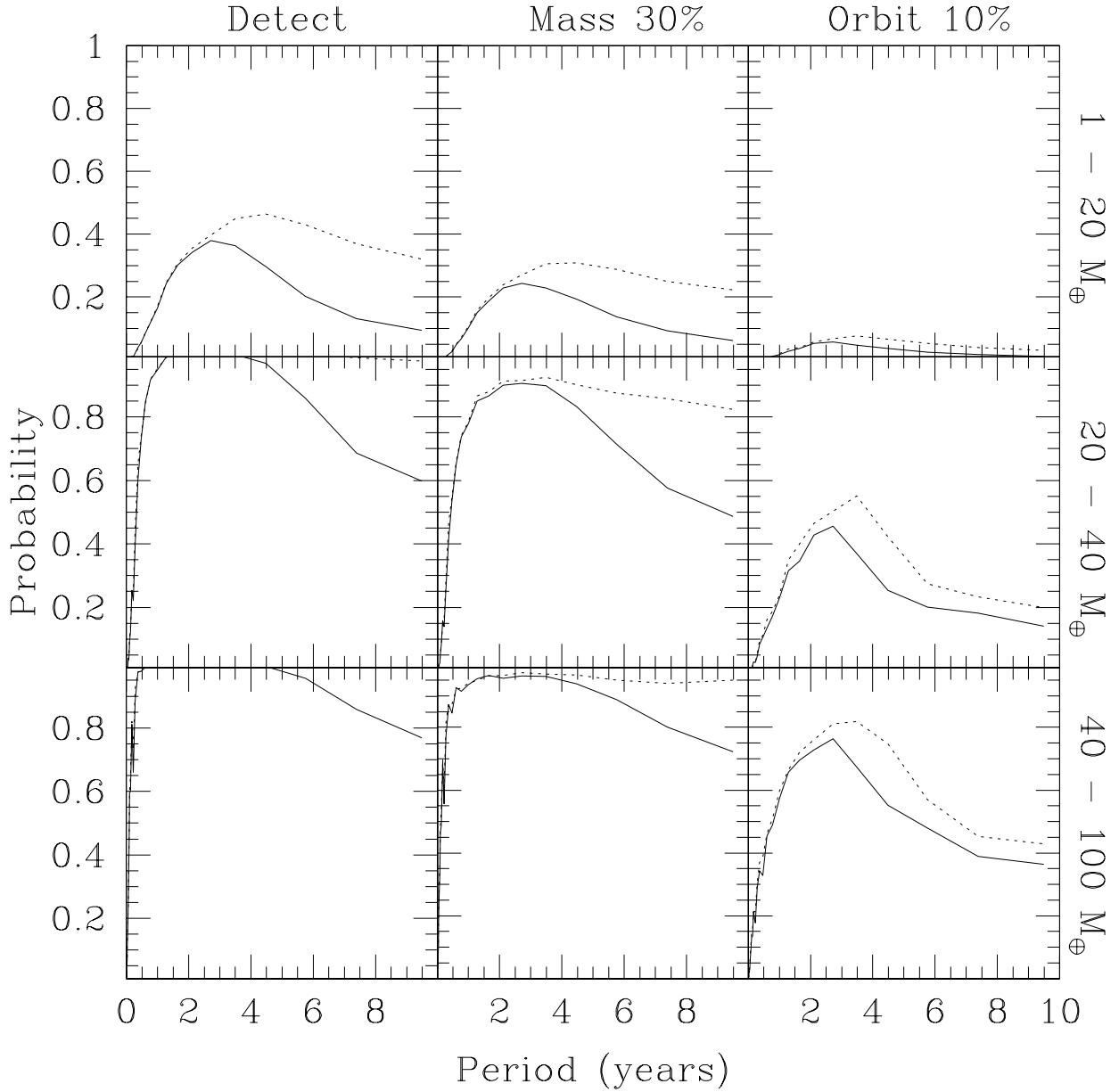
Fig. 4.— Here we show the rates for detecting and characterizing planets as a function of the planetary orbital period. In each panel the solid line is for models including an unknown constant acceleration and the dotted line assumes no acceleration. Each row of panels is for a different range of planetary masses (top: $1-20M_{\oplus}$, middle: $20-40M_{\oplus}$, bottom: $40-100M_{\oplus}$). The left column of panels is for detecting the planet, the center column is for measuring the mass with 30% accuracy, and the right column is for measuring the orbital parameters with 10% accuracy.
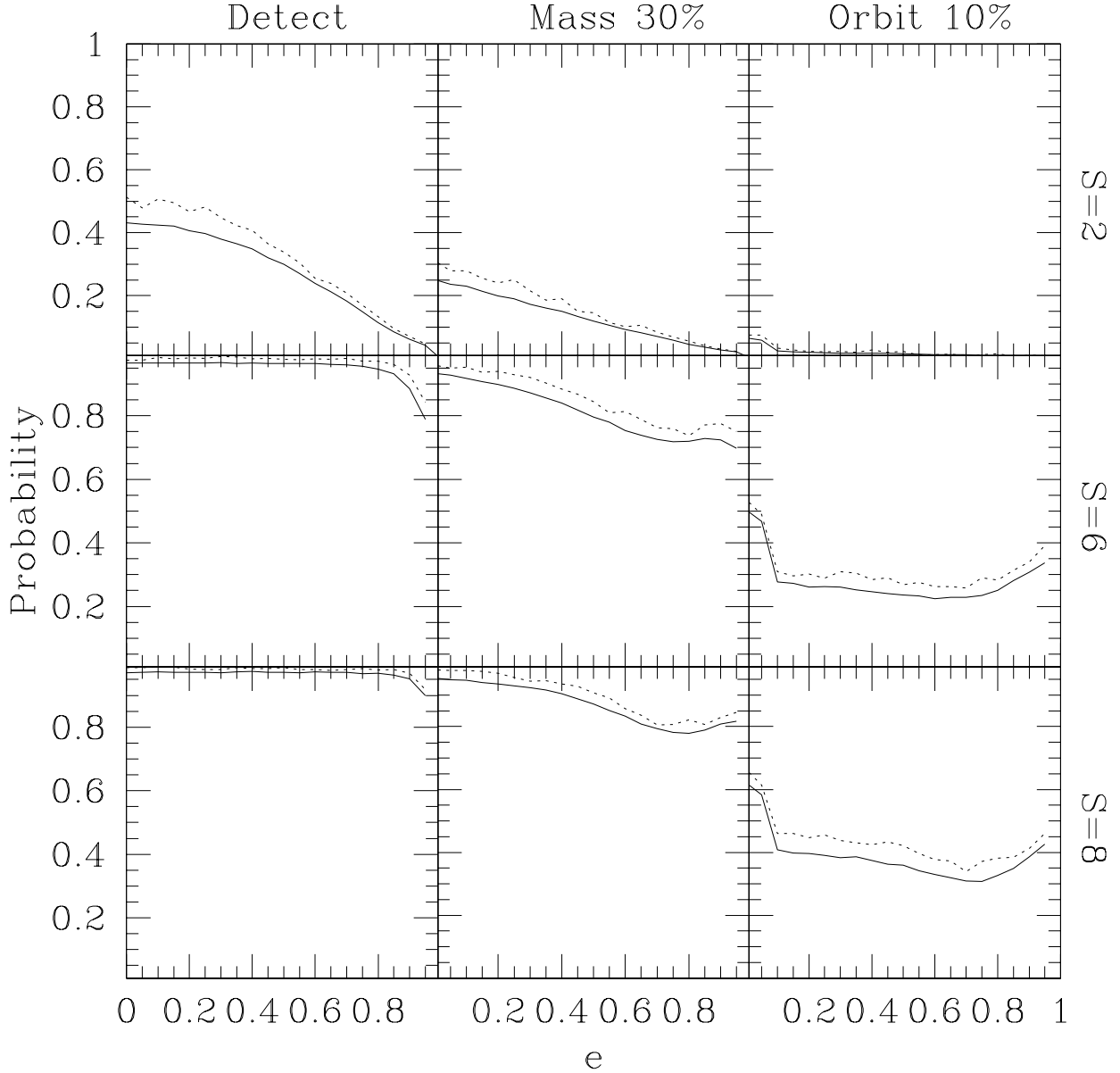
Fig. 5.— Here we show the rates for detecting and characterizing planets as a function of the planetary orbital eccentricity. In each panel the solid line is for models including an unknown constant acceleration and the dotted line assumes no acceleration. Each row of panels is for a different fixed value of the scaled signal (top: $S = 2$, middle: $S = 6$, bottom: $S = 8$). The left column of panels is for detecting the planet, the center column is for measuring the mass with 30% accuracy, and the right column is for measuring the orbital parameters with 10% accuracy.
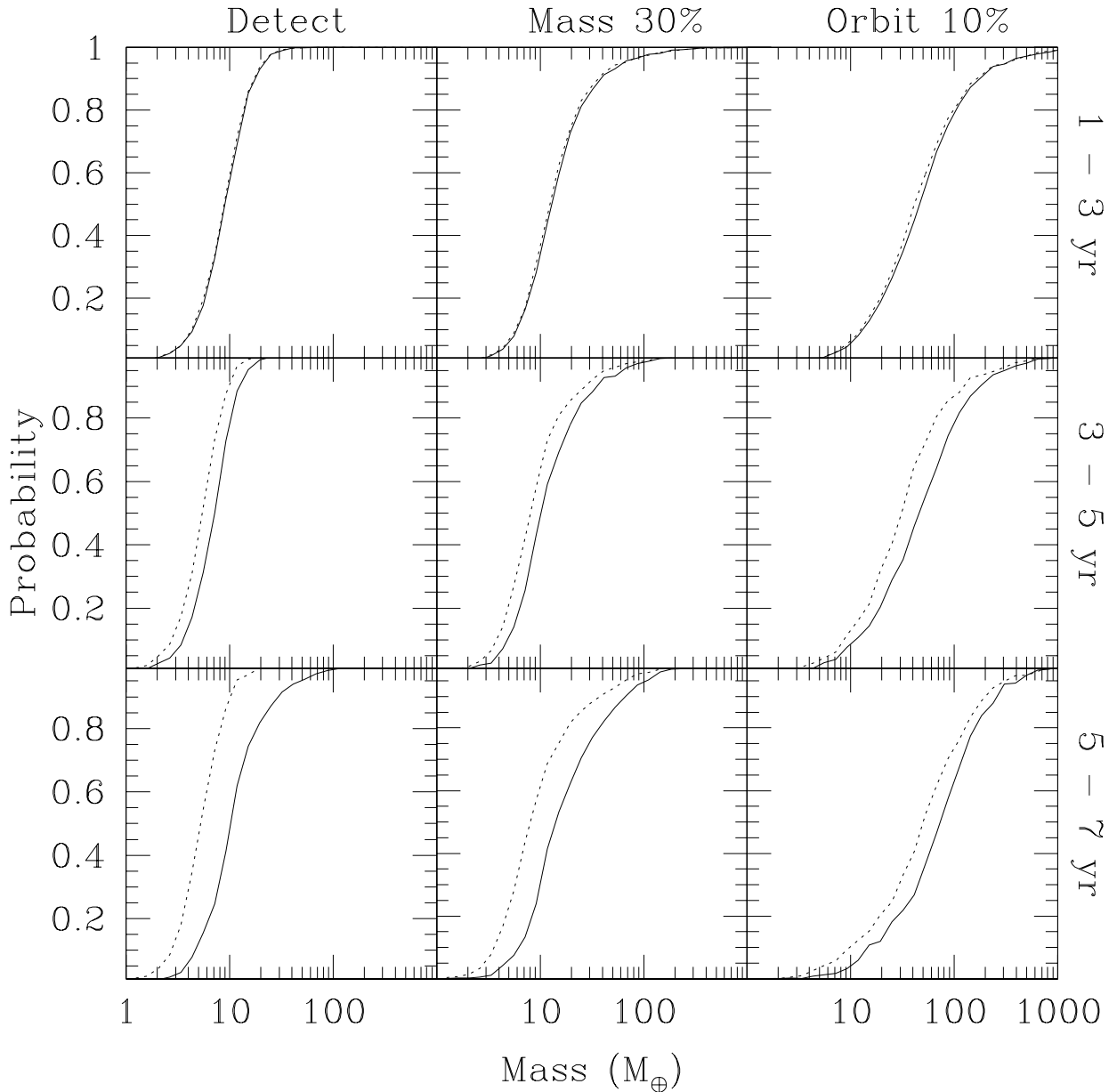
Fig. 6.— Here we show the rates for detecting and characterizing planets as a function of the planetary mass. In each panel the solid line is for models including an unknown constant acceleration and the dotted line assumes no acceleration. Each row of panels is for planets with orbital periods in a given range (top: 1-3 yr, middle: 3-5 yr, bottom: 5-7 yr). The left column of panels is for detecting the planet, the center column is for measuring the mass with 30% accuracy, and the right column is for measuring the orbital parameters with 10% accuracy.
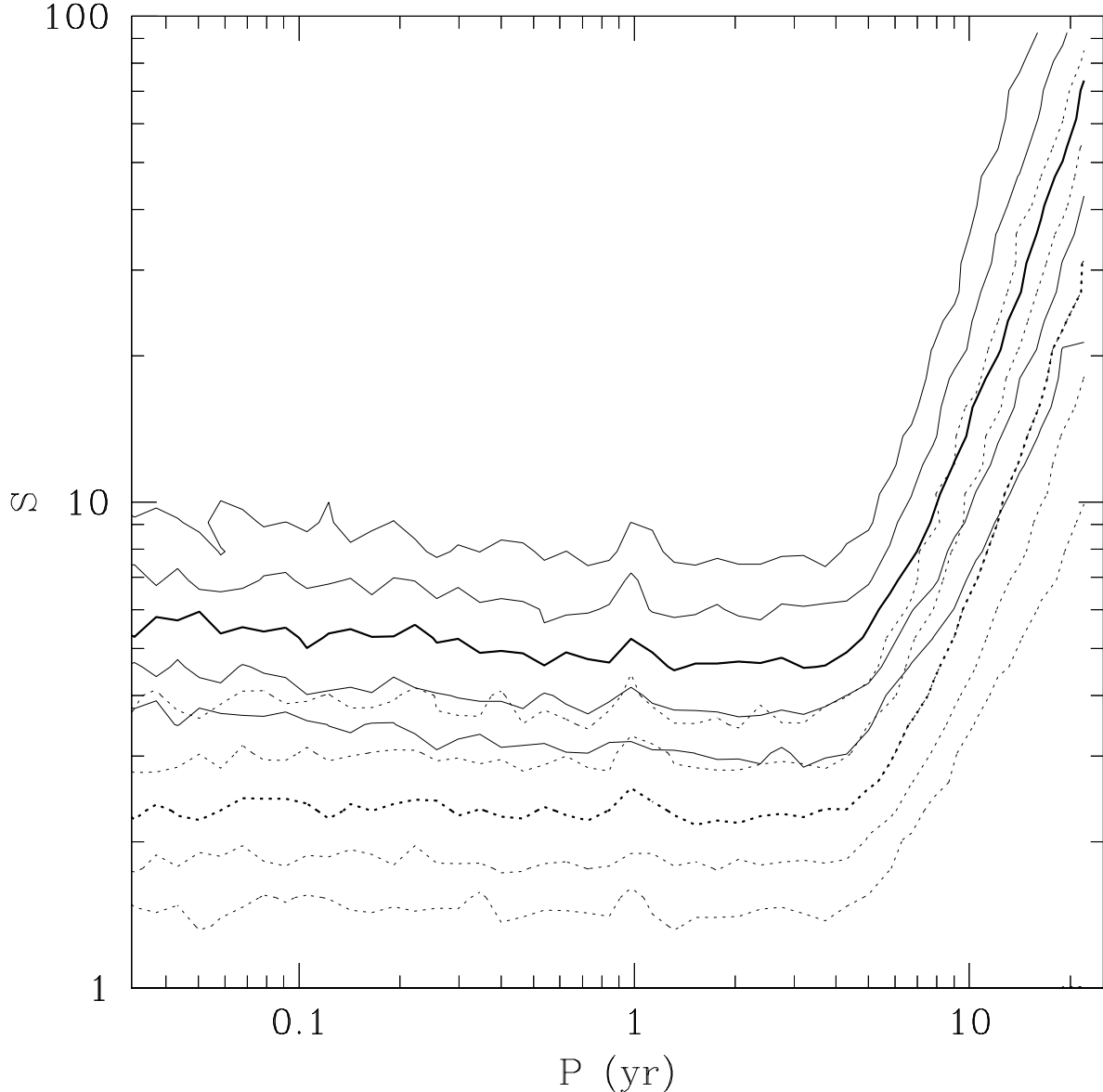
Fig. 7.— Here we show probability contours for detecting a single planet as a function of its orbital period and the scaled signal, averaging over the mass and other parameters. The contours are for 10%, 25%, 50% (bold), 75%, and 90% probability (bottom to top). The dotted lines are for rejecting the best-fit no-planet model with 99.9% probability. The solid lines also require that the reduction in χ^2 due to using the best-fit one-planet model is significant at the 99.9% level. These probability contours are similar to the probability contours for measuring the mass and orbital parameters with 30% accuracy 90% of the time (not shown).
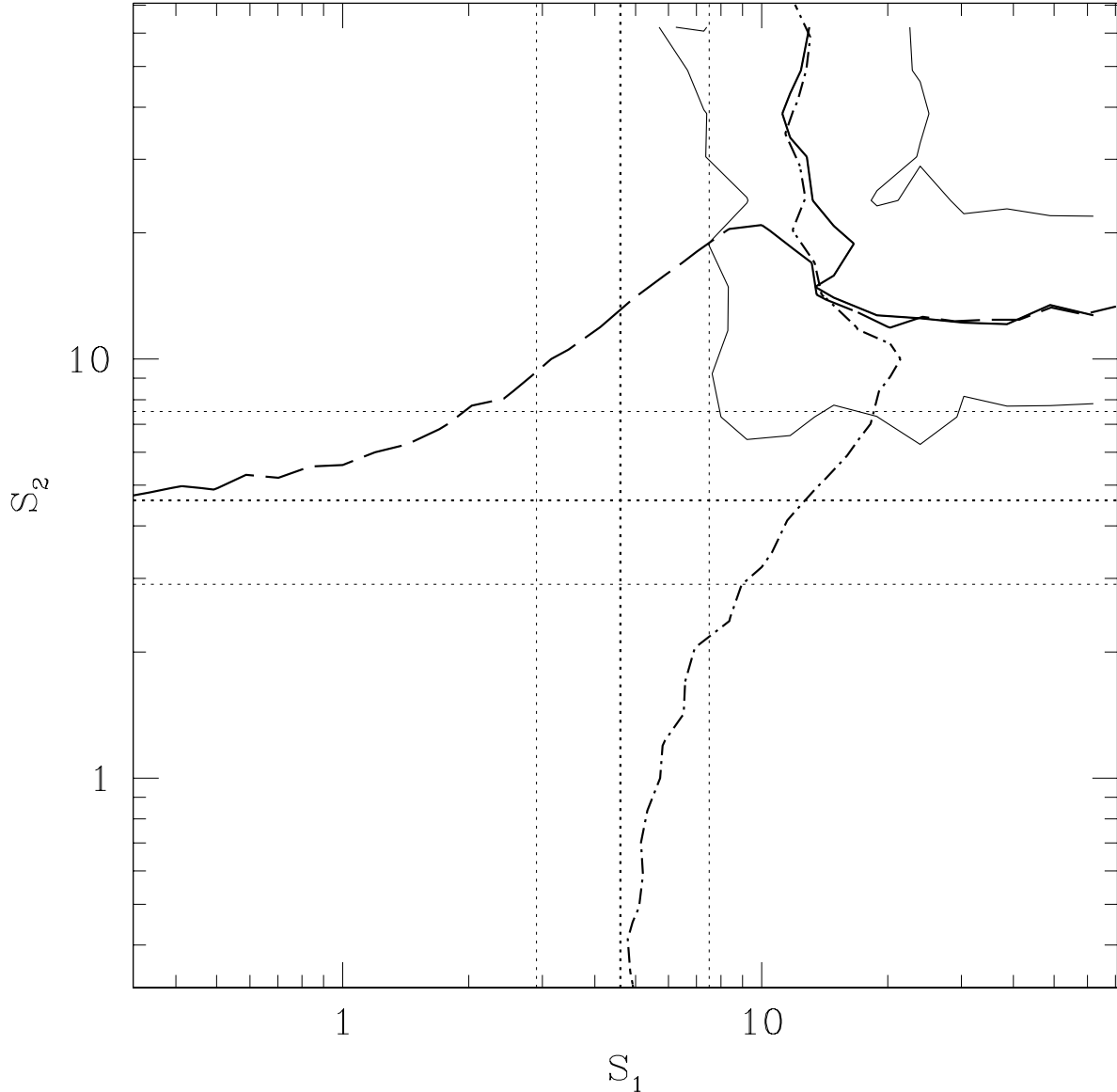
Fig. 8.— Here we show probability contours for detecting planets in a two-planet system as a function of their scaled signals, averaging over their masses, orbital periods (up to 5 years), and other parameters. The solid lines are for detecting both planets, and the dashed line and dotted-dashed line are for detecting either planet (regardless of whether the other planet is detected). The dotted lines are probability contours for detecting a single planet, if the other planet were not present. The contours are for 10%, 50% (bold), and 90% probability. Only the 50% contour is shown for detecting either planet individually.
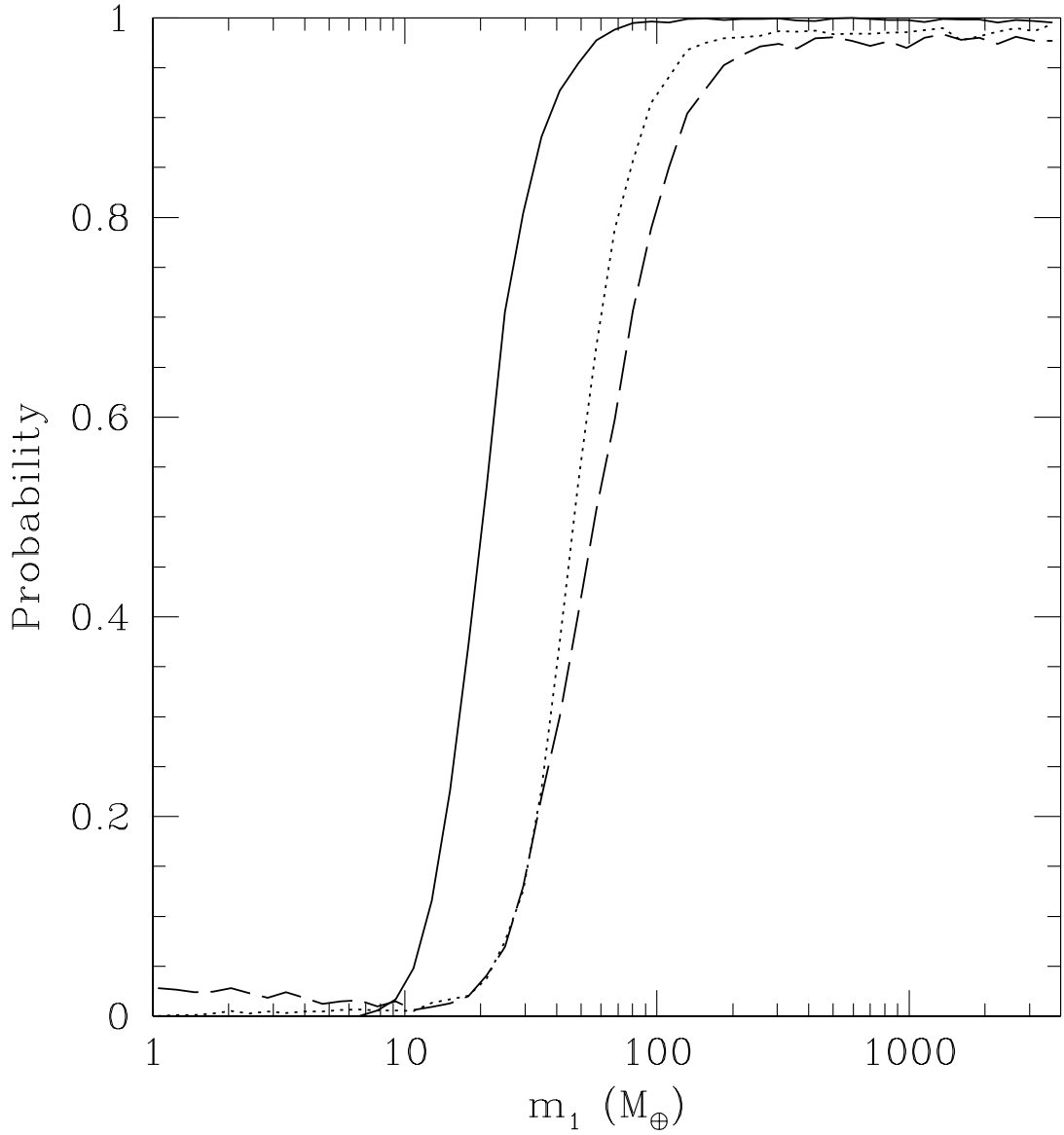
Fig. 9.— Here we show how the probability of detecting a planet is affected by the presence of a second planet in a long-period orbit. We plot the probability of detecting a planet (1) in a 1 year orbit as a function of the mass of that planet, m_1. The solid line is for a single planet, while the other lines are for a two planet system with a second planet in a 12 year orbit (dotted line: $m_2 = 1M_J$, dashed line: $m_2 = 20M_\oplus$). Note that these calculations assumed a distance of 10pc and 24 pairs of 1-d observations with single measurement precision of 1μas, but the results can be easily scaled to other distances and measurement precisions.
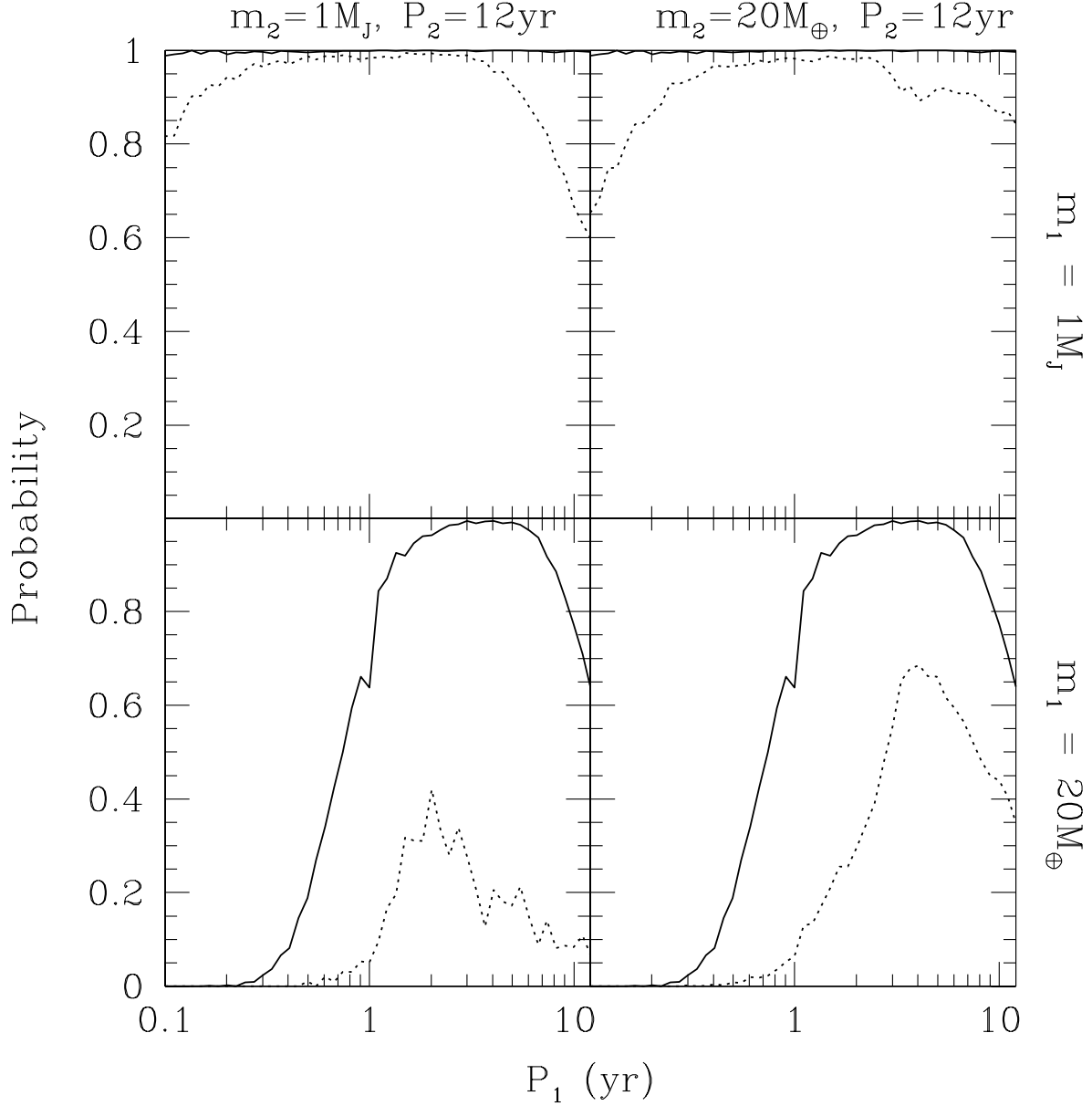
Fig. 10.— Here we show how the probability of detecting a planet is affected by the presence of a second planet in a long-period orbit. We plot the probability of detecting a planet (1) as a function of that planet's orbital period, P_1. The different rows of panels are for detecting a planet of different masses (top row: $m_1 = 1M_J$, bottom row: $m_1 = 20M_\oplus$). The solid lines are for a single planet, and the dotted lines are for a two planet system. The left column of panels is for a second planet with mass $m_2 = 1M_J$, and the right column of panels is for a second planet with mass $m_2 = 20M_\oplus$.
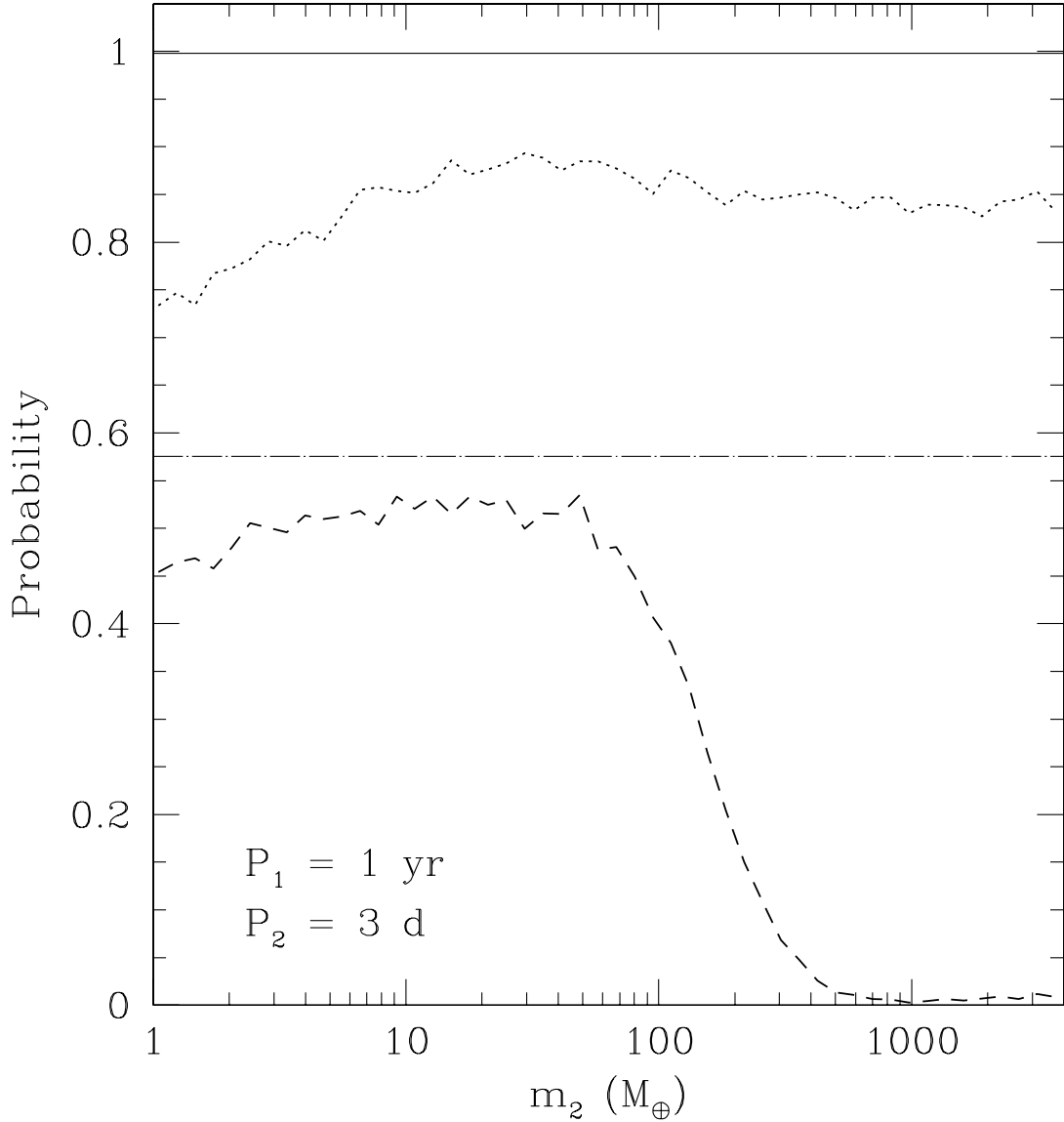
Fig. 11.— Here we show how the probability of detecting a planet is affected by the presence of a second planet in a short-period orbit. We plot the probability of detecting a planet (1) in a 1 year orbit as a function of the mass of the short-period planet, m_2. The solid and dotted-dashed lines are for the outer planet in isolation, while the other lines are for a two planet system with a second planet in a 3 day orbit. The top pair of lines is for $m_1 = 1M_J$, and the bottom pair of lines is for $m_1 = 20M_\oplus$.
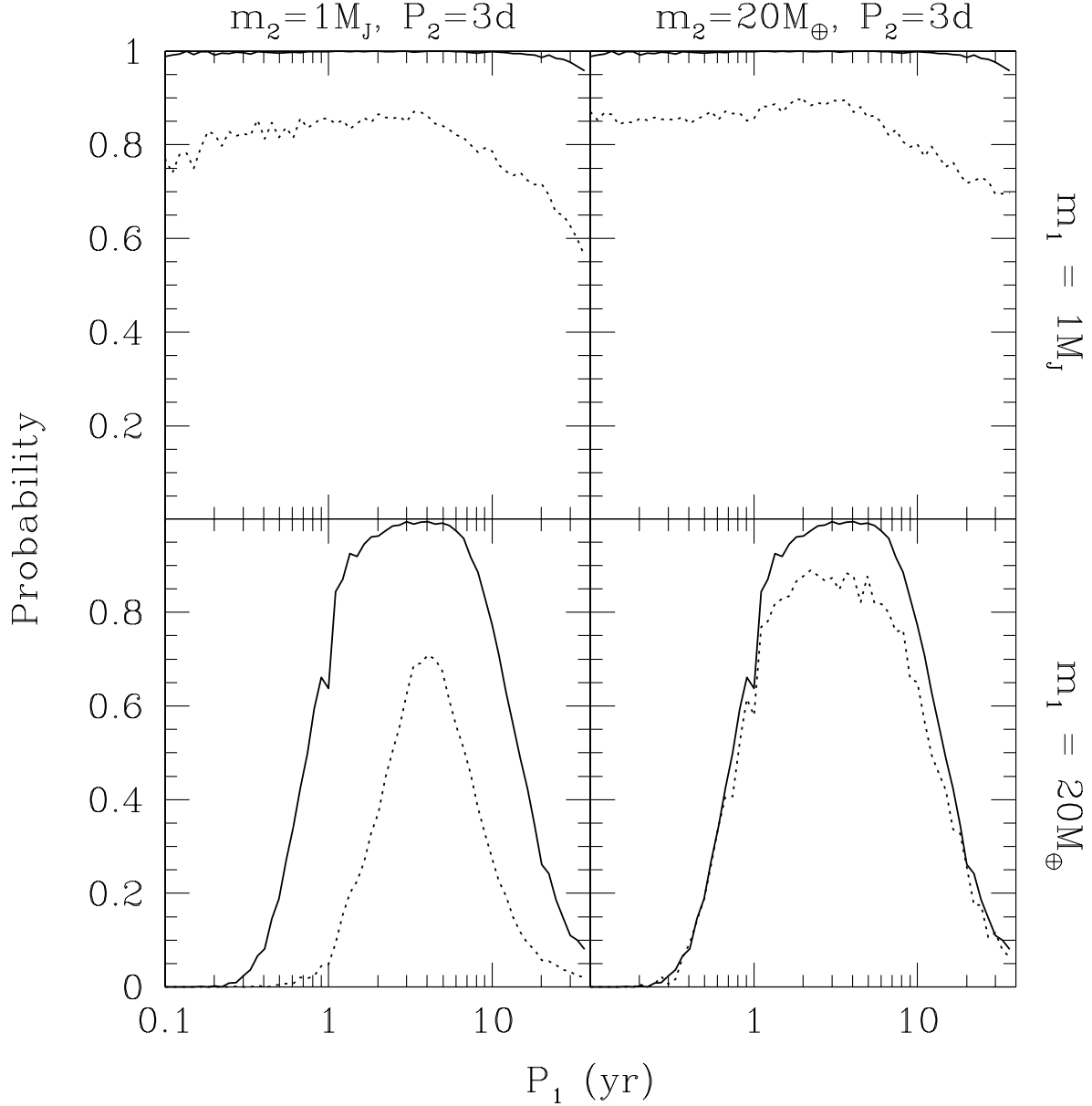
Fig. 12.— Here we show how the probability of detecting a planet is affected by the presence of a second planet in a short-period orbit. We plot the probability of detecting a planet (1) as a function of the orbital period of that planet, P_1. The different rows of panels are for detecting a planet of different masses (top row: $m_1 = 1M_J$, bottom row: $m_1 = 20M_\oplus$). The solid lines are for a single planet, while the dotted lines are for a two-planet system with a second planet in a 3 day orbit. The left column of panels is for a second planet with mass $m_2 = 1M_J$, and the right column of panels is for a second planet with mass $m_2 = 20M_\oplus$.
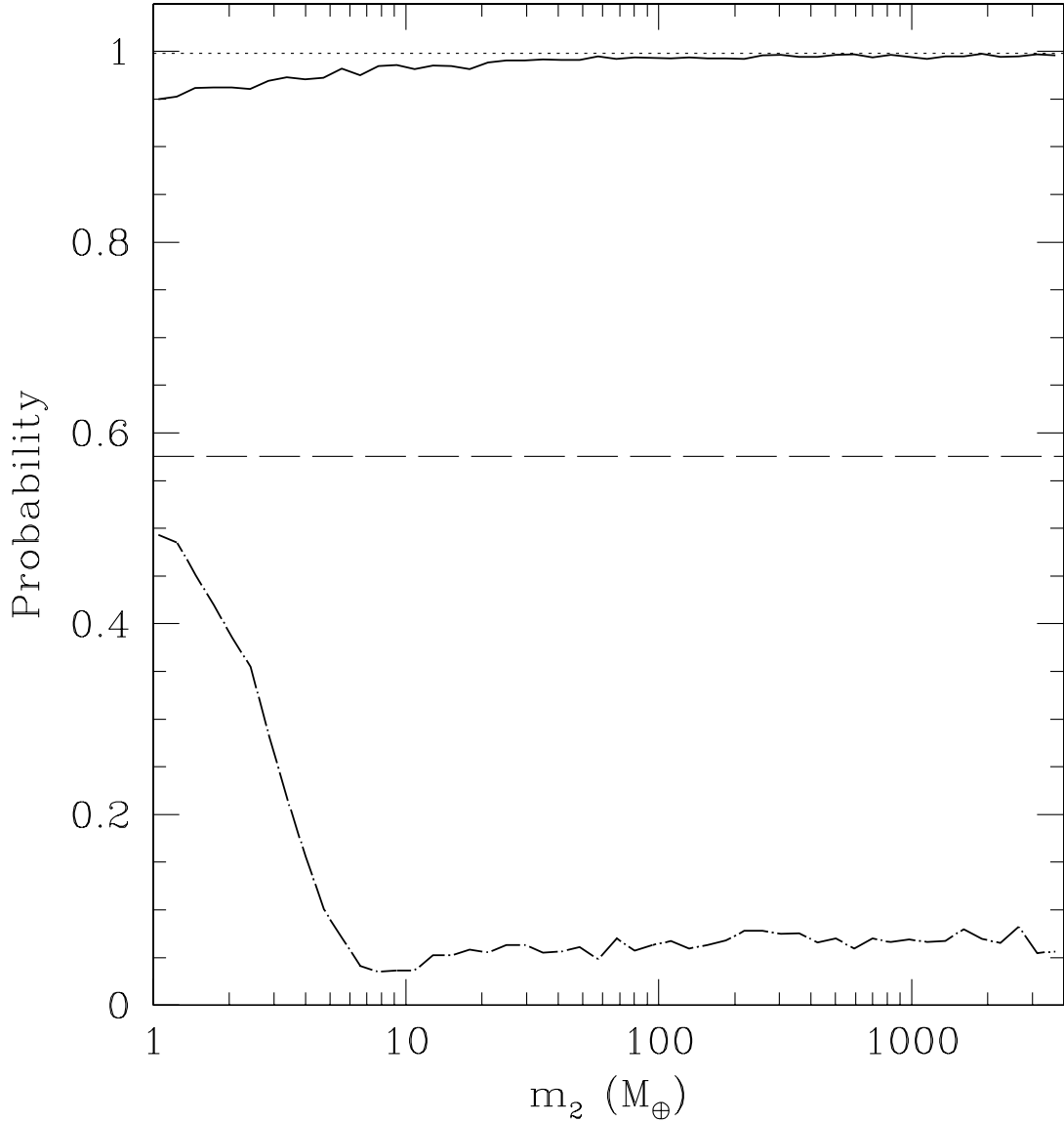
Fig. 13.— Here we show how the probability of detecting a planet is affected by the presence of a second nearby planet. We plot the probability of detecting a planet (1) in a 1 year orbit as a function of the mass of a second planet, m_2 in a 3 year orbit. For reference, the horizontal lines show the probability for detecting the inner planet in isolation. The other lines are for a two-planet system with a second planet in a 3 year orbit. The top pair of lines is for $m_1 = 1 M_J$, and the bottom pair of lines is for $m_1 = 20 M_\oplus$.
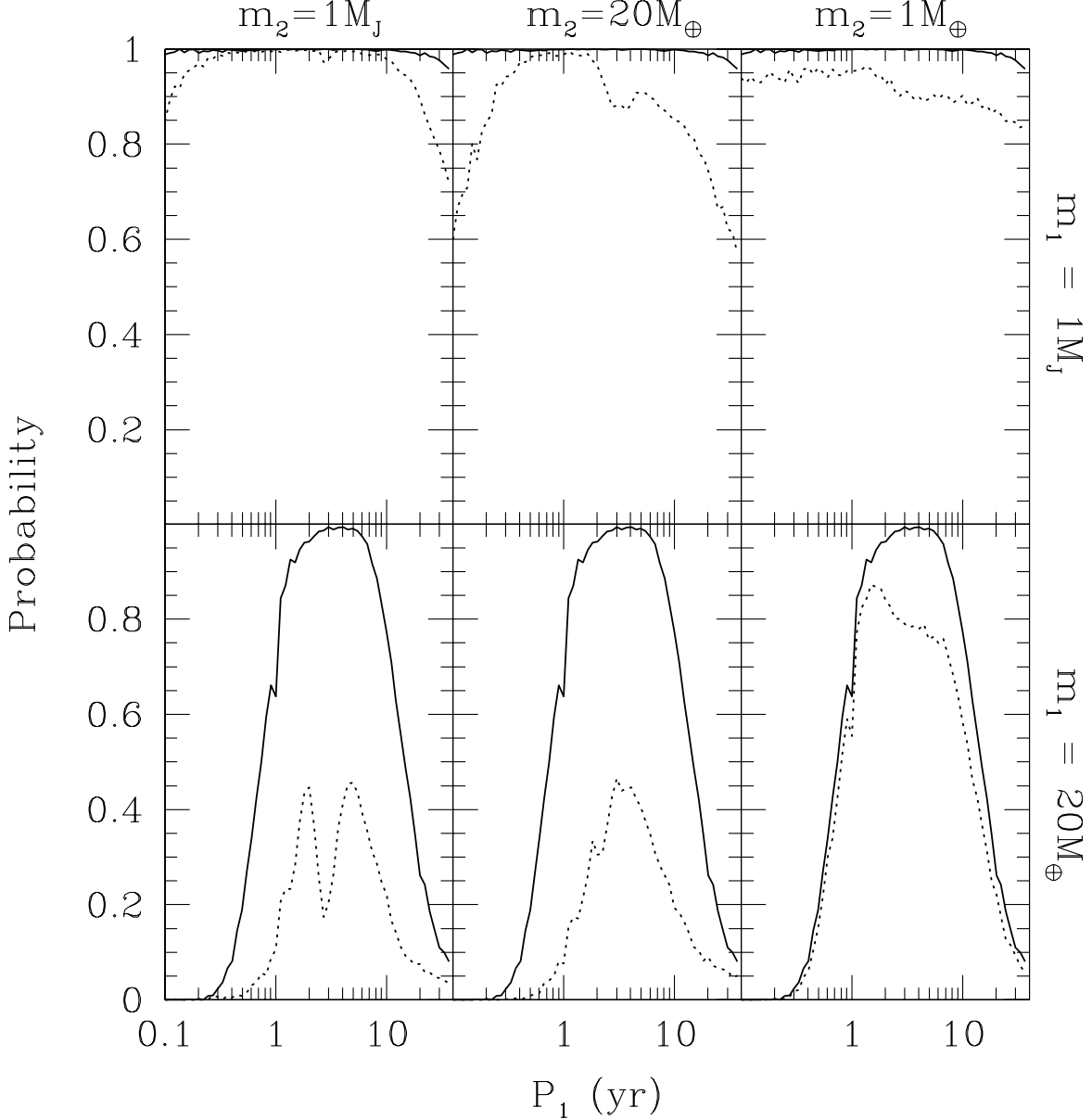
Fig. 14.— Here we show how the probability of detecting a planet is affected by the presence of a second nearby planet. We plot the probability of detecting a planet (1) as a function of the orbital period of that planet, P_1. The different rows of panels are for detecting a planet of different masses (top row: $m_1 = 1M_J$, bottom row: $m_1 = 20M_\oplus$). The solid lines are for a single planet, while the dotted lines are for a two planet system with a second planet in a 3 year orbit. The left column of panels is for a second planet with mass $m_2 = 1M_J$, the center column of panels is for a second planet with mass $m_2 = 20M_\oplus$, and the right column of panels is for a second planet with mass $m_2 = 1M_\oplus$.
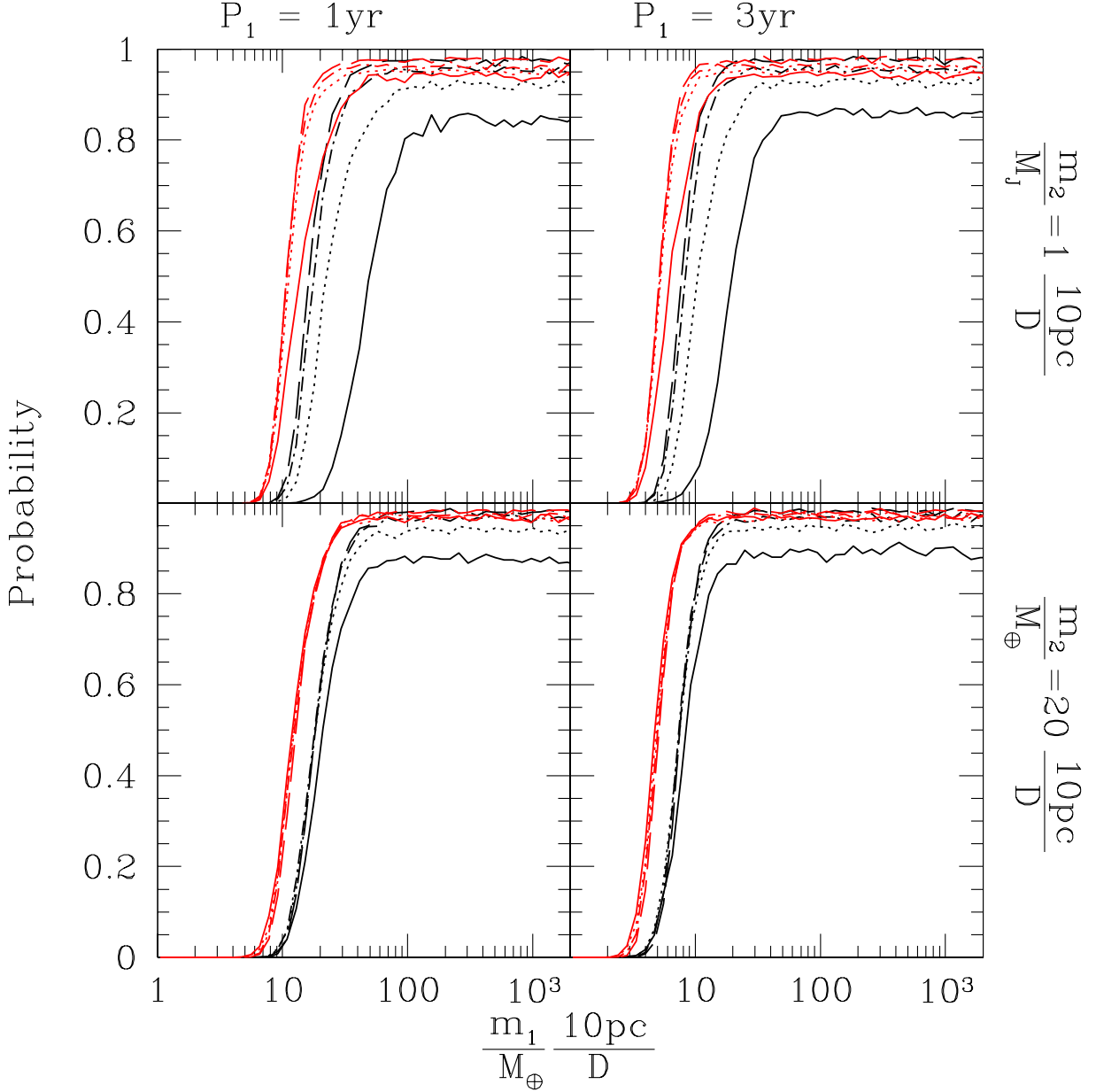
Fig. 15.— Here we show how the probability of detecting a planet in the presence of a second planet in a short-period orbit is improved by adding radial velocity observations. We plot the probability of detecting a planet (1) in a 1yr (left panels) or 3yr (right panels) period orbit as a function of its mass (m_1). The second planet is in a 3d orbit has a mass of $1M_J$ (top panels) or $20M_\oplus$ (bottom panels). These results can be scaled to different planet masses and stellar distances, as indicated by the x-axis label and the panel labels on the right. The solid lines a for a survey with only 24 2-d astrometric observations. The remaining lines are for a survey including 24 2-d astrometric observations and 12 (dotted), 24 (dotted-dashed), or 48 (long dashed) radial velocity observations with 3m/s precision. The electronic version includes red curves that assume 48 2-d astrometric observations over a 10 year mission.
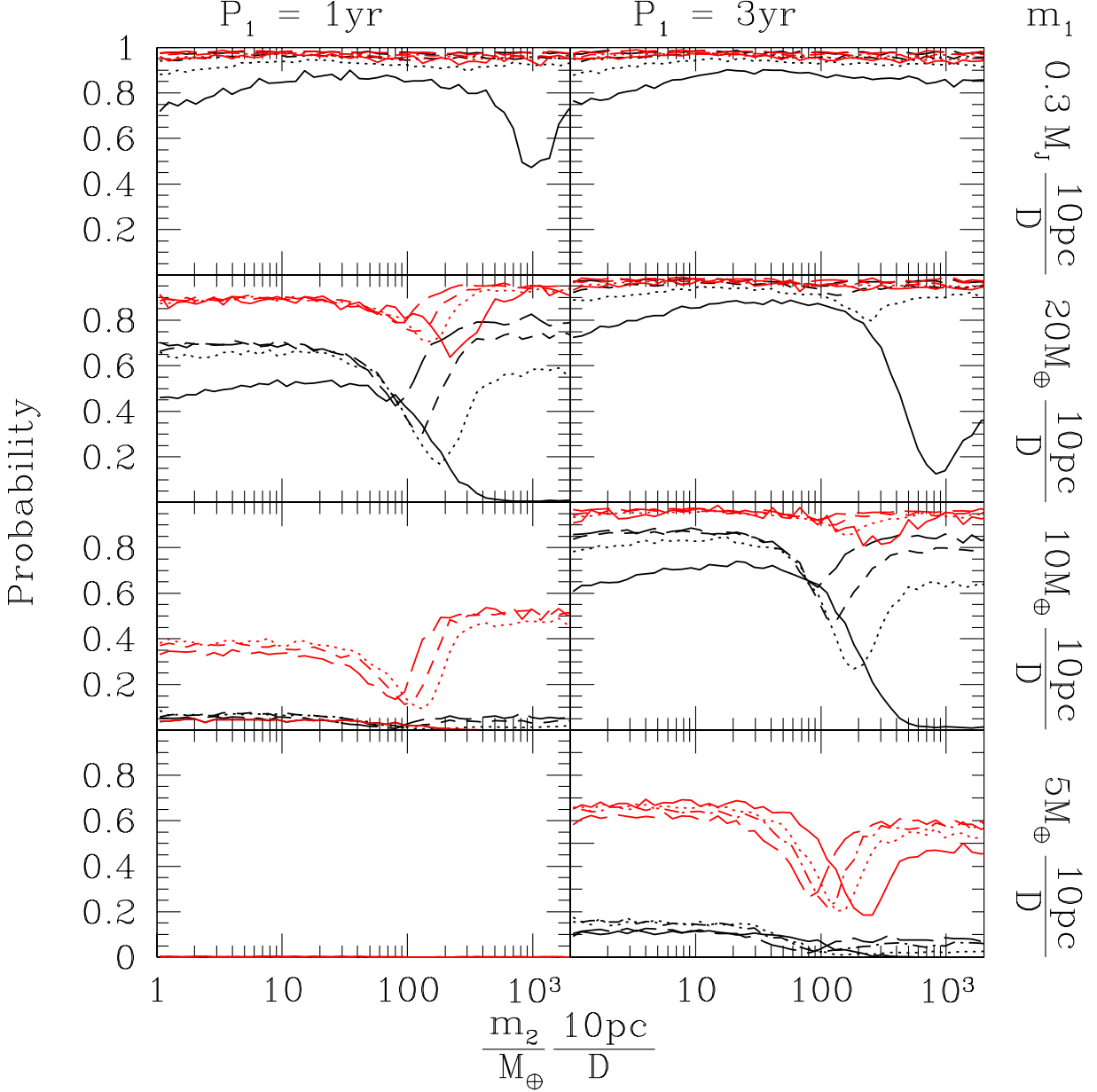
Fig. 16.— Here we show how the probability of detecting a planet in the presence of a second planet in a short-period orbit is improved by adding radial velocity observations. We plot the probability of detecting a planet of mass $0.3M_J$ (top panels), $20M_\oplus$ (upper middle panels), $10M_\oplus$ (lower middle panels), or $5M_\oplus$ (bottom panels) in a 1yr (left panels) or 3yr (right panels) period orbit as a function of the mass of the short-period planet (m_2) in a 3d orbit. These results can be scaled to different planet masses and stellar distances, as indicated by the x-axis label and the panel labels on the right. The solid lines a for a survey with only 24 2-d astrometric observations. The remaining lines are for a survey including 24 2-d astrometric observations and 12 (dotted), 24 (dotted-dashed), or 48 (long dashed) radial velocity observations with 3m/s precision. The electronic version includes red curves that assume 48 2-d astrometric observations over a 10 year mission.

Table 1.

Mass		Period		One Planet		Two Planets		
A	B	A	B	A	B	A	B	A&B
5 $M_\oplus$	5 $M_\oplus$	3 d	60 d	0.00	0.00	-	-	0.00
5 $M_\oplus$	10 $M_\oplus$	3 d	60 d	0.00	0.00	-	-	0.00
5 $M_\oplus$	20 $M_\oplus$	3 d	60 d	0.00	0.00	-	-	0.00
5 $M_\oplus$	0.3 M_J	3 d	60 d	0.00	0.91	-	0.82	0.00
5 $M_\oplus$	1 M_J	3 d	60 d	0.00	1.00	-	0.81	0.00
10 $M_\oplus$	5 $M_\oplus$	3 d	60 d	0.00	0.00	-	-	0.00
10 $M_\oplus$	10 $M_\oplus$	3 d	60 d	0.00	0.00	-	-	0.00
10 $M_\oplus$	20 $M_\oplus$	3 d	60 d	0.00	0.00	-	-	0.00
10 $M_\oplus$	0.3 M_J	3 d	60 d	0.00	0.91	-	0.86	0.00
10 $M_\oplus$	1 M_J	3 d	60 d	0.00	1.00	-	0.84	0.00
20 $M_\oplus$	5 $M_\oplus$	3 d	60 d	0.00	0.00	-	-	0.00
20 $M_\oplus$	10 $M_\oplus$	3 d	60 d	0.00	0.00	-	-	0.00
20 $M_\oplus$	20 $M_\oplus$	3 d	60 d	0.00	0.00	-	-	0.00
20 $M_\oplus$	0.3 M_J	3 d	60 d	0.00	0.91	-	0.87	0.00
20 $M_\oplus$	1 M_J	3 d	60 d	0.00	1.00	-	0.86	0.00
0.3 M_J	5 $M_\oplus$	3 d	60 d	0.00	0.00	-	-	0.00
0.3 M_J	10 $M_\oplus$	3 d	60 d	0.00	0.00	-	-	0.00
0.3 M_J	20 $M_\oplus$	3 d	60 d	0.00	0.00	-	-	0.00
0.3 M_J	0.3 M_J	3 d	60 d	0.00	0.91	-	0.80	0.00
0.3 M_J	1 M_J	3 d	60 d	0.00	1.00	-	0.84	0.00
1 M_J	5 $M_\oplus$	3 d	60 d	0.11	0.00	0.87	-	0.00
1 M_J	10 $M_\oplus$	3 d	60 d	0.11	0.00	0.62	-	0.00
1 M_J	20 $M_\oplus$	3 d	60 d	0.11	0.00	0.16	-	0.00
1 M_J	0.3 M_J	3 d	60 d	0.11	0.91	0.00	0.21	0.00
1 M_J	1 M_J	3 d	60 d	0.11	1.00	0.00	0.82	0.00
5 $M_\oplus$	5 $M_\oplus$	3 d	1 yr	0.00	0.00	-	-	0.00
5 $M_\oplus$	10 $M_\oplus$	3 d	1 yr	0.00	0.04	-	0.98	0.00
5 $M_\oplus$	20 $M_\oplus$	3 d	1 yr	0.00	0.58	-	0.90	0.00
5 $M_\oplus$	0.3 M_J	3 d	1 yr	0.00	1.00	-	0.82	0.00
5 $M_\oplus$	1 M_J	3 d	1 yr	0.00	1.00	-	0.83	0.00
10 $M_\oplus$	5 $M_\oplus$	3 d	1 yr	0.00	0.00	-	-	0.00
10 $M_\oplus$	10 $M_\oplus$	3 d	1 yr	0.00	0.04	-	0.97	0.00

Table 1—Continued

Mass		Period		One Planet		Two Planets		
A	B	A	B	A	B	A	B	A&B
10 $M_\oplus$	20 $M_\oplus$	3 d	1 yr	0.00	0.58	-	0.91	0.00
10 $M_\oplus$	0.3 M_J	3 d	1 yr	0.00	1.00	-	0.86	0.00
10 $M_\oplus$	1 M_J	3 d	1 yr	0.00	1.00	-	0.86	0.00
20 $M_\oplus$	5 $M_\oplus$	3 d	1 yr	0.00	0.00	-	-	0.00
20 $M_\oplus$	10 $M_\oplus$	3 d	1 yr	0.00	0.04	-	0.97	0.00
20 $M_\oplus$	20 $M_\oplus$	3 d	1 yr	0.00	0.58	-	0.90	0.00
20 $M_\oplus$	0.3 M_J	3 d	1 yr	0.00	1.00	-	0.88	0.00
20 $M_\oplus$	1 M_J	3 d	1 yr	0.00	1.00	-	0.88	0.00
0.3 M_J	5 $M_\oplus$	3 d	1 yr	0.00	0.00	-	-	0.00
0.3 M_J	10 $M_\oplus$	3 d	1 yr	0.00	0.04	-	0.51	0.00
0.3 M_J	20 $M_\oplus$	3 d	1 yr	0.00	0.58	-	0.66	0.00
0.3 M_J	0.3 M_J	3 d	1 yr	0.00	1.00	-	0.86	0.00
0.3 M_J	1 M_J	3 d	1 yr	0.00	1.00	-	0.86	0.00
1 M_J	5 $M_\oplus$	3 d	1 yr	0.11	0.00	0.22	-	0.00
1 M_J	10 $M_\oplus$	3 d	1 yr	0.11	0.04	0.03	0.03	0.00
1 M_J	20 $M_\oplus$	3 d	1 yr	0.11	0.58	0.00	0.07	0.00
1 M_J	0.3 M_J	3 d	1 yr	0.11	1.00	0.00	0.81	0.00
1 M_J	1 M_J	3 d	1 yr	0.11	1.00	0.00	0.85	0.00
5 $M_\oplus$	5 $M_\oplus$	3 d	3 yr	0.00	0.12	-	0.93	0.00
5 $M_\oplus$	10 $M_\oplus$	3 d	3 yr	0.00	0.79	-	0.87	0.00
5 $M_\oplus$	20 $M_\oplus$	3 d	3 yr	0.00	0.99	-	0.85	0.00
5 $M_\oplus$	0.3 M_J	3 d	3 yr	0.00	1.00	-	0.84	0.00
5 $M_\oplus$	1 M_J	3 d	3 yr	0.00	1.00	-	0.85	0.00
10 $M_\oplus$	5 $M_\oplus$	3 d	3 yr	0.00	0.12	-	0.97	0.00
10 $M_\oplus$	10 $M_\oplus$	3 d	3 yr	0.00	0.79	-	0.91	0.00
10 $M_\oplus$	20 $M_\oplus$	3 d	3 yr	0.00	0.99	-	0.88	0.00
10 $M_\oplus$	0.3 M_J	3 d	3 yr	0.00	1.00	-	0.88	0.00
10 $M_\oplus$	1 M_J	3 d	3 yr	0.00	1.00	-	0.87	0.00
20 $M_\oplus$	5 $M_\oplus$	3 d	3 yr	0.00	0.12	-	0.96	0.00
20 $M_\oplus$	10 $M_\oplus$	3 d	3 yr	0.00	0.79	-	0.92	0.00
20 $M_\oplus$	20 $M_\oplus$	3 d	3 yr	0.00	0.99	-	0.89	0.00
20 $M_\oplus$	0.3 M_J	3 d	3 yr	0.00	1.00	-	0.89	0.00

Table 1—Continued

Mass		Period		One Planet		Two Planets		
A	B	A	B	A	B	A	B	A&B
20 $M_\oplus$	1 M_J	3 d	3 yr	0.00	1.00	-	0.89	0.00
0.3 M_J	5 $M_\oplus$	3 d	3 yr	0.00	0.12	-	0.47	0.00
0.3 M_J	10 $M_\oplus$	3 d	3 yr	0.00	0.79	-	0.75	0.00
0.3 M_J	20 $M_\oplus$	3 d	3 yr	0.00	0.99	-	0.87	0.00
0.3 M_J	0.3 M_J	3 d	3 yr	0.00	1.00	-	0.88	0.00
0.3 M_J	1 M_J	3 d	3 yr	0.00	1.00	-	0.88	0.00
1 M_J	5 $M_\oplus$	3 d	3 yr	0.11	0.12	0.02	0.02	0.00
1 M_J	10 $M_\oplus$	3 d	3 yr	0.11	0.79	0.00	0.11	0.00
1 M_J	20 $M_\oplus$	3 d	3 yr	0.11	0.99	0.00	0.59	0.00
1 M_J	0.3 M_J	3 d	3 yr	0.11	1.00	0.00	0.85	0.00
1 M_J	1 M_J	3 d	3 yr	0.11	1.00	0.00	0.87	0.00
5 $M_\oplus$	5 $M_\oplus$	3 d	12 yr	0.00	0.04	-	0.91	0.00
5 $M_\oplus$	10 $M_\oplus$	3 d	12 yr	0.00	0.31	-	0.87	0.00
5 $M_\oplus$	20 $M_\oplus$	3 d	12 yr	0.00	0.68	-	0.79	0.00
5 $M_\oplus$	0.3 M_J	3 d	12 yr	0.00	0.99	-	0.75	0.00
5 $M_\oplus$	1 M_J	3 d	12 yr	0.00	1.00	-	0.74	0.00
10 $M_\oplus$	5 $M_\oplus$	3 d	12 yr	0.00	0.04	-	0.99	0.00
10 $M_\oplus$	10 $M_\oplus$	3 d	12 yr	0.00	0.31	-	0.88	0.00
10 $M_\oplus$	20 $M_\oplus$	3 d	12 yr	0.00	0.68	-	0.82	0.00
10 $M_\oplus$	0.3 M_J	3 d	12 yr	0.00	0.99	-	0.77	0.00
10 $M_\oplus$	1 M_J	3 d	12 yr	0.00	1.00	-	0.77	0.00
20 $M_\oplus$	5 $M_\oplus$	3 d	12 yr	0.00	0.04	-	0.90	0.00
20 $M_\oplus$	10 $M_\oplus$	3 d	12 yr	0.00	0.31	-	0.88	0.00
20 $M_\oplus$	20 $M_\oplus$	3 d	12 yr	0.00	0.68	-	0.83	0.00
20 $M_\oplus$	0.3 M_J	3 d	12 yr	0.00	0.99	-	0.78	0.00
20 $M_\oplus$	1 M_J	3 d	12 yr	0.00	1.00	-	0.78	0.00
0.3 M_J	5 $M_\oplus$	3 d	12 yr	0.00	0.04	-	0.56	0.00
0.3 M_J	10 $M_\oplus$	3 d	12 yr	0.00	0.31	-	0.68	0.00
0.3 M_J	20 $M_\oplus$	3 d	12 yr	0.00	0.68	-	0.74	0.00
0.3 M_J	0.3 M_J	3 d	12 yr	0.00	0.99	-	0.77	0.00
0.3 M_J	1 M_J	3 d	12 yr	0.00	1.00	-	0.77	0.00
1 M_J	5 $M_\oplus$	3 d	12 yr	0.11	0.04	0.19	0.03	0.00

Table 1—Continued

Mass		Period		One Planet		Two Planets		
A	B	A	B	A	B	A	B	A&B
$1\ M_J$	$10\ M_\oplus$	3 d	12 yr	0.11	0.31	0.05	0.11	0.00
$1\ M_J$	$20\ M_\oplus$	3 d	12 yr	0.11	0.68	0.00	0.32	0.00
$1\ M_J$	$0.3\ M_J$	3 d	12 yr	0.11	0.99	0.00	0.71	0.00
$1\ M_J$	$1\ M_J$	3 d	12 yr	0.11	1.00	0.00	0.76	0.00
$5\ M_\oplus$	$5\ M_\oplus$	60 d	1 yr	0.00	0.00	-	-	0.00
$5\ M_\oplus$	$10\ M_\oplus$	60 d	1 yr	0.00	0.04	-	0.86	0.00
$5\ M_\oplus$	$20\ M_\oplus$	60 d	1 yr	0.00	0.58	-	0.92	0.00
$5\ M_\oplus$	$0.3\ M_J$	60 d	1 yr	0.00	1.00	-	0.94	0.00
$5\ M_\oplus$	$1\ M_J$	60 d	1 yr	0.00	1.00	-	0.95	0.00
$10\ M_\oplus$	$5\ M_\oplus$	60 d	1 yr	0.00	0.00	-	-	0.00
$10\ M_\oplus$	$10\ M_\oplus$	60 d	1 yr	0.00	0.04	-	0.63	0.00
$10\ M_\oplus$	$20\ M_\oplus$	60 d	1 yr	0.00	0.58	-	0.82	0.00
$10\ M_\oplus$	$0.3\ M_J$	60 d	1 yr	0.00	1.00	-	0.96	0.00
$10\ M_\oplus$	$1\ M_J$	60 d	1 yr	0.00	1.00	-	0.96	0.00
$20\ M_\oplus$	$5\ M_\oplus$	60 d	1 yr	0.00	0.00	-	-	0.00
$20\ M_\oplus$	$10\ M_\oplus$	60 d	1 yr	0.00	0.04	-	0.22	0.00
$20\ M_\oplus$	$20\ M_\oplus$	60 d	1 yr	0.00	0.58	-	0.50	0.00
$20\ M_\oplus$	$0.3\ M_J$	60 d	1 yr	0.00	1.00	-	0.96	0.00
$20\ M_\oplus$	$1\ M_J$	60 d	1 yr	0.00	1.00	-	0.96	0.00
$0.3\ M_J$	$5\ M_\oplus$	60 d	1 yr	0.91	0.00	0.85	-	0.00
$0.3\ M_J$	$10\ M_\oplus$	60 d	1 yr	0.91	0.04	0.52	0.01	0.00
$0.3\ M_J$	$20\ M_\oplus$	60 d	1 yr	0.91	0.58	0.12	0.04	0.02
$0.3\ M_J$	$0.3\ M_J$	60 d	1 yr	0.91	1.00	0.16	0.72	0.15
$0.3\ M_J$	$1\ M_J$	60 d	1 yr	0.91	1.00	0.17	0.98	0.15
$1\ M_J$	$5\ M_\oplus$	60 d	1 yr	1.00	0.00	0.96	-	0.00
$1\ M_J$	$10\ M_\oplus$	60 d	1 yr	1.00	0.04	0.96	0.01	0.00
$1\ M_J$	$20\ M_\oplus$	60 d	1 yr	1.00	0.58	0.92	0.03	0.02
$1\ M_J$	$0.3\ M_J$	60 d	1 yr	1.00	1.00	0.94	0.92	0.91
$1\ M_J$	$1\ M_J$	60 d	1 yr	1.00	1.00	0.96	0.98	0.95
$5\ M_\oplus$	$5\ M_\oplus$	60 d	3 yr	0.00	0.12	-	0.88	0.00
$5\ M_\oplus$	$10\ M_\oplus$	60 d	3 yr	0.00	0.79	-	0.95	0.00
$5\ M_\oplus$	$20\ M_\oplus$	60 d	3 yr	0.00	0.99	-	0.95	0.00

Table 1—Continued

Mass		Period		One Planet		Two Planets		
A	B	A	B	A	B	A	B	A&B
5 $M_\oplus$	0.3 M_J	60 d	3 yr	0.00	1.00	-	0.96	0.00
5 $M_\oplus$	1 M_J	60 d	3 yr	0.00	1.00	-	0.95	0.00
10 $M_\oplus$	5 $M_\oplus$	60 d	3 yr	0.00	0.12	-	0.63	0.00
10 $M_\oplus$	10 $M_\oplus$	60 d	3 yr	0.00	0.79	-	0.88	0.00
10 $M_\oplus$	20 $M_\oplus$	60 d	3 yr	0.00	0.99	-	0.95	0.00
10 $M_\oplus$	0.3 M_J	60 d	3 yr	0.00	1.00	-	0.96	0.00
10 $M_\oplus$	1 M_J	60 d	3 yr	0.00	1.00	-	0.97	0.00
20 $M_\oplus$	5 $M_\oplus$	60 d	3 yr	0.00	0.12	-	0.21	0.00
20 $M_\oplus$	10 $M_\oplus$	60 d	3 yr	0.00	0.79	-	0.62	0.00
20 $M_\oplus$	20 $M_\oplus$	60 d	3 yr	0.00	0.99	-	0.94	0.00
20 $M_\oplus$	0.3 M_J	60 d	3 yr	0.00	1.00	-	0.97	0.00
20 $M_\oplus$	1 M_J	60 d	3 yr	0.00	1.00	-	0.98	0.00
0.3 M_J	5 $M_\oplus$	60 d	3 yr	0.91	0.12	0.41	0.02	0.00
0.3 M_J	10 $M_\oplus$	60 d	3 yr	0.91	0.79	0.10	0.07	0.05
0.3 M_J	20 $M_\oplus$	60 d	3 yr	0.91	0.99	0.18	0.27	0.16
0.3 M_J	0.3 M_J	60 d	3 yr	0.91	1.00	0.20	0.98	0.18
0.3 M_J	1 M_J	60 d	3 yr	0.91	1.00	0.19	0.99	0.18
1 M_J	5 $M_\oplus$	60 d	3 yr	1.00	0.12	0.97	0.02	0.00
1 M_J	10 $M_\oplus$	60 d	3 yr	1.00	0.79	0.91	0.08	0.06
1 M_J	20 $M_\oplus$	60 d	3 yr	1.00	0.99	0.82	0.59	0.59
1 M_J	0.3 M_J	60 d	3 yr	1.00	1.00	0.96	0.98	0.96
1 M_J	1 M_J	60 d	3 yr	1.00	1.00	0.96	0.99	0.96
5 $M_\oplus$	5 $M_\oplus$	60 d	12 yr	0.00	0.04	-	0.89	0.00
5 $M_\oplus$	10 $M_\oplus$	60 d	12 yr	0.00	0.31	-	0.91	0.00
5 $M_\oplus$	20 $M_\oplus$	60 d	12 yr	0.00	0.68	-	0.89	0.00
5 $M_\oplus$	0.3 M_J	60 d	12 yr	0.00	0.99	-	0.89	0.00
5 $M_\oplus$	1 M_J	60 d	12 yr	0.00	1.00	-	0.89	0.00
10 $M_\oplus$	5 $M_\oplus$	60 d	12 yr	0.00	0.04	-	0.70	0.00
10 $M_\oplus$	10 $M_\oplus$	60 d	12 yr	0.00	0.31	-	0.81	0.00
10 $M_\oplus$	20 $M_\oplus$	60 d	12 yr	0.00	0.68	-	0.88	0.00
10 $M_\oplus$	0.3 M_J	60 d	12 yr	0.00	0.99	-	0.90	0.00
10 $M_\oplus$	1 M_J	60 d	12 yr	0.00	1.00	-	0.91	0.00

Table 1—Continued

Mass		Period		One Planet		Two Planets		
A	B	A	B	A	B	A	B	A&B
20 $M_\oplus$	5 $M_\oplus$	60 d	12 yr	0.00	0.04	-	0.31	0.00
20 $M_\oplus$	10 $M_\oplus$	60 d	12 yr	0.00	0.31	-	0.54	0.00
20 $M_\oplus$	20 $M_\oplus$	60 d	12 yr	0.00	0.68	-	0.75	0.00
20 $M_\oplus$	0.3 M_J	60 d	12 yr	0.00	0.99	-	0.92	0.00
20 $M_\oplus$	1 M_J	60 d	12 yr	0.00	1.00	-	0.93	0.00
0.3 M_J	5 $M_\oplus$	60 d	12 yr	0.91	0.04	0.68	0.03	0.00
0.3 M_J	10 $M_\oplus$	60 d	12 yr	0.91	0.31	0.37	0.05	0.01
0.3 M_J	20 $M_\oplus$	60 d	12 yr	0.91	0.68	0.18	0.15	0.06
0.3 M_J	0.3 M_J	60 d	12 yr	0.91	0.99	0.13	0.75	0.12
0.3 M_J	1 M_J	60 d	12 yr	0.91	1.00	0.13	0.94	0.12
1 M_J	5 $M_\oplus$	60 d	12 yr	1.00	0.04	0.94	0.03	0.00
1 M_J	10 $M_\oplus$	60 d	12 yr	1.00	0.31	0.92	0.07	0.02
1 M_J	20 $M_\oplus$	60 d	12 yr	1.00	0.68	0.85	0.28	0.19
1 M_J	0.3 M_J	60 d	12 yr	1.00	0.99	0.90	0.88	0.85
1 M_J	1 M_J	60 d	12 yr	1.00	1.00	0.94	0.96	0.93
5 $M_\oplus$	5 $M_\oplus$	1 yr	3 yr	0.00	0.12	-	0.37	0.00
5 $M_\oplus$	10 $M_\oplus$	1 yr	3 yr	0.00	0.79	-	0.73	0.00
5 $M_\oplus$	20 $M_\oplus$	1 yr	3 yr	0.00	0.99	-	0.94	0.00
5 $M_\oplus$	0.3 M_J	1 yr	3 yr	0.00	1.00	-	0.95	0.00
5 $M_\oplus$	1 M_J	1 yr	3 yr	0.00	1.00	-	0.96	0.00
10 $M_\oplus$	5 $M_\oplus$	1 yr	3 yr	0.04	0.12	0.04	0.08	0.00
10 $M_\oplus$	10 $M_\oplus$	1 yr	3 yr	0.04	0.79	0.06	0.31	0.00
10 $M_\oplus$	20 $M_\oplus$	1 yr	3 yr	0.04	0.99	0.12	0.85	0.00
10 $M_\oplus$	0.3 M_J	1 yr	3 yr	0.04	1.00	0.49	0.96	0.00
10 $M_\oplus$	1 M_J	1 yr	3 yr	0.04	1.00	0.50	0.96	0.00
20 $M_\oplus$	5 $M_\oplus$	1 yr	3 yr	0.58	0.12	0.11	0.03	0.00
20 $M_\oplus$	10 $M_\oplus$	1 yr	3 yr	0.58	0.79	0.07	0.09	0.04
20 $M_\oplus$	20 $M_\oplus$	1 yr	3 yr	0.58	0.99	0.10	0.43	0.06
20 $M_\oplus$	0.3 M_J	1 yr	3 yr	0.58	1.00	0.11	0.98	0.05
20 $M_\oplus$	1 M_J	1 yr	3 yr	0.58	1.00	0.12	0.97	0.05
0.3 M_J	5 $M_\oplus$	1 yr	3 yr	1.00	0.12	0.96	0.04	0.00
0.3 M_J	10 $M_\oplus$	1 yr	3 yr	1.00	0.79	0.84	0.14	0.11

Table 1—Continued

Mass		Period		One Planet		Two Planets		
A	B	A	B	A	B	A	B	A&B
0.3 M_J	20 $M_\oplus$	1 yr	3 yr	1.00	0.99	0.83	0.68	0.67
0.3 M_J	0.3 M_J	1 yr	3 yr	1.00	1.00	0.95	0.99	0.95
0.3 M_J	1 M_J	1 yr	3 yr	1.00	1.00	0.95	0.99	0.94
1 M_J	5 $M_\oplus$	1 yr	3 yr	1.00	0.12	0.98	0.04	0.00
1 M_J	10 $M_\oplus$	1 yr	3 yr	1.00	0.79	0.98	0.15	0.11
1 M_J	20 $M_\oplus$	1 yr	3 yr	1.00	0.99	0.99	0.69	0.69
1 M_J	0.3 M_J	1 yr	3 yr	1.00	1.00	1.00	0.99	0.99
1 M_J	1 M_J	1 yr	3 yr	1.00	1.00	1.00	1.00	1.00
5 $M_\oplus$	5 $M_\oplus$	1 yr	12 yr	0.00	0.04	-	0.35	0.00
5 $M_\oplus$	10 $M_\oplus$	1 yr	12 yr	0.00	0.31	-	0.64	0.00
5 $M_\oplus$	0.3 M_J	1 yr	12 yr	0.00	0.99	-	0.91	0.00
10 $M_\oplus$	5 $M_\oplus$	1 yr	12 yr	0.04	0.04	0.27	0.09	0.00
10 $M_\oplus$	10 $M_\oplus$	1 yr	12 yr	0.04	0.31	0.12	0.26	0.00
10 $M_\oplus$	0.3 M_J	1 yr	12 yr	0.04	0.99	0.52	0.91	0.00
20 $M_\oplus$	5 $M_\oplus$	1 yr	12 yr	0.58	0.04	0.43	0.01	0.00
20 $M_\oplus$	10 $M_\oplus$	1 yr	12 yr	0.58	0.31	0.17	0.07	0.01
20 $M_\oplus$	20 $M_\oplus$	1 yr	12 yr	0.58	0.68	0.08	0.23	0.02
20 $M_\oplus$	0.3 M_J	1 yr	12 yr	0.58	0.99	0.09	0.84	0.03
20 $M_\oplus$	1 M_J	1 yr	12 yr	0.58	1.00	0.07	0.96	0.03
0.3 M_J	5 $M_\oplus$	1 yr	12 yr	1.00	0.04	0.95	0.05	0.00
0.3 M_J	10 $M_\oplus$	1 yr	12 yr	1.00	0.31	0.90	0.14	0.04
0.3 M_J	0.3 M_J	1 yr	12 yr	1.00	0.99	0.92	0.91	0.88
1 M_J	5 $M_\oplus$	1 yr	12 yr	1.00	0.04	0.96	0.06	0.00
1 M_J	10 $M_\oplus$	1 yr	12 yr	1.00	0.31	0.97	0.13	0.04
1 M_J	20 $M_\oplus$	1 yr	12 yr	1.00	0.68	0.98	0.37	0.25
1 M_J	0.3 M_J	1 yr	12 yr	1.00	0.99	0.99	0.92	0.91
1 M_J	1 M_J	1 yr	12 yr	1.00	1.00	0.99	0.98	0.98
5 $M_\oplus$	5 $M_\oplus$	3 yr	12 yr	0.12	0.04	0.72	0.81	0.00
5 $M_\oplus$	10 $M_\oplus$	3 yr	12 yr	0.12	0.31	0.99	0.47	0.00
5 $M_\oplus$	20 $M_\oplus$	3 yr	12 yr	0.12	0.68	1.42	0.50	0.00
5 $M_\oplus$	0.3 M_J	3 yr	12 yr	0.12	0.99	1.12	0.81	0.00
5 $M_\oplus$	1 M_J	3 yr	12 yr	0.12	1.00	0.41	0.91	0.00

Table 1—Continued

| Mass | | Period | | One Planet | | Two Planets | | |
A	B	A	B	A	B	A	B	A&B
10 $M_\oplus$	5 $M_\oplus$	3 yr	12 yr	0.79	0.04	0.66	1.37	0.00
10 $M_\oplus$	10 $M_\oplus$	3 yr	12 yr	0.79	0.31	0.44	0.30	0.00
10 $M_\oplus$	20 $M_\oplus$	3 yr	12 yr	0.79	0.68	0.32	0.32	0.01
10 $M_\oplus$	0.3 M_J	3 yr	12 yr	0.79	0.99	0.24	0.71	0.01
10 $M_\oplus$	1 M_J	3 yr	12 yr	0.79	1.00	0.11	0.89	0.01
20 $M_\oplus$	5 $M_\oplus$	3 yr	12 yr	0.99	0.04	0.85	1.30	0.00
20 $M_\oplus$	10 $M_\oplus$	3 yr	12 yr	0.99	0.31	0.74	0.25	0.01
20 $M_\oplus$	20 $M_\oplus$	3 yr	12 yr	0.99	0.68	0.54	0.23	0.05
20 $M_\oplus$	0.3 M_J	3 yr	12 yr	0.99	0.99	0.41	0.63	0.20
20 $M_\oplus$	1 M_J	3 yr	12 yr	0.99	1.00	0.30	0.84	0.18
0.3 M_J	5 $M_\oplus$	3 yr	12 yr	1.00	0.04	0.93	0.87	0.00
0.3 M_J	10 $M_\oplus$	3 yr	12 yr	1.00	0.31	0.93	0.19	0.02
0.3 M_J	20 $M_\oplus$	3 yr	12 yr	1.00	0.68	0.93	0.25	0.13
0.3 M_J	0.3 M_J	3 yr	12 yr	1.00	0.99	0.97	0.80	0.77
0.3 M_J	1 M_J	3 yr	12 yr	1.00	1.00	0.98	0.96	0.95
1 M_J	5 $M_\oplus$	3 yr	12 yr	1.00	0.04	0.96	0.16	0.00
1 M_J	10 $M_\oplus$	3 yr	12 yr	1.00	0.31	0.96	0.10	0.01
1 M_J	20 $M_\oplus$	3 yr	12 yr	1.00	0.68	0.96	0.21	0.12
1 M_J	0.3 M_J	3 yr	12 yr	1.00	0.99	0.98	0.81	0.80
1 M_J	1 M_J	3 yr	12 yr	1.00	1.00	0.99	0.97	0.97

Note. —